

~~CONFIDENTIAL~~

NACA RM A54D19

6432

TECHNICAL LIBRARY

NACA

AF 7291

0143345

TECH LIBRARY KAFB, NM

RESEARCH MEMORANDUM

PRESSURE DISTRIBUTIONS ON TRIANGULAR AND RECTANGULAR

WINGS TO HIGH ANGLES OF ATTACK -

MACH NUMBERS 1.45 AND 1.97

By George E. Kaattari

Ames Aeronautical Laboratory
Moffett Field, Calif.Classification and Control (changed to Unclassified)By NASA Tech Rep Announcement #33
(OFFICER MAKING CHANGE)By 24 Nov. 60
NAME ANDNIS
GRADE OF OFFICER MAKING CHANGE)8 Feb. 61
DATE

CLASSIFIED DOCUMENT

This material contains information affecting the National Defense of the United States within the meaning of the espionage laws, Title 18, U.S.C., Secs. 793 and 794, the transmission or revelation of which in any manner to an unauthorized person is prohibited by law.

NATIONAL ADVISORY COMMITTEE
FOR AERONAUTICS

WASHINGTON

June 25, 1954

~~CONFIDENTIAL~~



NATIONAL ADVISORY COMMITTEE FOR AERONAUTICS

RESEARCH MEMORANDUMPRESSURE DISTRIBUTIONS ON TRIANGULAR AND RECTANGULAR
WINGS TO HIGH ANGLES OF ATTACK -

MACH NUMBERS 1.45 AND 1.97

By George E. Kaattari

SUMMARY

In order to provide detailed wing-load-distribution data to high angles of attack, semispan pressure-distribution models of triangular and rectangular plan forms were tested at Mach number 1.45 within the angle-of-attack range of 0° to 30° and at Mach number 1.97 within the angle-of-attack range of 0° to 50° . The tests were made at Reynolds numbers of 0.26×10^6 per inch and 0.44×10^6 per inch for both Mach numbers.

Data were obtained on five models. The three basic models were two triangular wings of aspect ratios 2 and 4 and one rectangular wing of aspect ratio 2, all having thickened root sections, a structural feature generally required for supersonic all-movable wings. To evaluate the possible aerodynamic penalty of thickening the root sections, two other aspect-ratio-2 models, identical to two of the basic models but without thickened root sections, were provided.

In all cases the wings showed a tendency toward uniform loading at high angles of attack. Thus, as the angle of attack was increased, the center of pressure moved toward the centroid of area or, in terms of spanwise location, the center of pressure moved outboard for the rectangular wings and inboard for the triangular wings. The presence of thickened root sections on the wings had little effect on the centers of pressure and normal-force coefficients. Reynolds number effects were negligible in the range tested except for a small reduction in normal force in the case of the rectangular wing with thickened root at $M = 1.97$ as the Reynolds number was reduced from 1.76×10^6 to 1.04×10^6 .

INTRODUCTION

Since wings and controls for supersonic interceptor aircraft maneuvering at high altitudes are required to operate over a wide range of angles of attack, information is required on wing load distribution at large as well as small angles of attack. Unfortunately, available theory on the aerodynamic behavior of wing and wing-body configurations at supersonic speeds is restricted to cases where the angle of attack is small. Detailed pressure-distribution data on wing-body components available in the literature (e.g., refs. 1 to 3) are also generally limited to small angles of attack. Little data are available for high angles of attack at supersonic speeds, particularly for wing-body models with variable-incidence wings. In an effort to provide data for high angles of attack, a program has been initiated to measure pressure distribution through a wide range of angles of attack, both on wing-body combinations and on the components (wing and body). It is hoped that the data obtained will not only provide needed design information, but will also point the way for development of theories applicable over a wide range of angles of attack.

The present report presents pressure-distribution data to high angles of attack for several wings at two supersonic Mach numbers. The following data are presented: (1) tabulated pressure coefficients, (2) span-load-distribution curves for each angle of attack, (3) curves of normal force as a function of angle of attack, and (4) curves of center-of-pressure position as a function of angle of attack.

NOTATION

- A wing aspect ratio
- C_m pitching-moment coefficient, $\frac{C_N(x_h - \bar{x})}{\bar{c}}$
- C_N normal-force coefficient, $\frac{N}{qS}$
- c local chord, in.
- c_n local normal-force coefficient
- c_r root chord, in.
- \bar{c} mean aerodynamic chord, $\frac{\int_0^S c^2 dy}{\int_0^S c dy}$, in.

cc_n	span loading coefficient, in.
M	free-stream Mach number
N	normal force, lb
P	pressure coefficient, $\frac{p - p_o}{q}$
p	orifice static pressure, lb/sq in.
p_o	free-stream static pressure, lb/sq in.
p_w	reference static pressure, lb/sq in.
q	free-stream dynamic pressure, lb/sq in.
R	Reynolds number, per in.
s	wing semispan, in.
S	wing area, in. ²
W	wing (Subscript denotes model.)
x	chordwise distance from leading edge at spanwise distance y , in.
x_h	distance from leading edge to hinge line along root chord, in.
\bar{x}	distance from leading edge to wing center of pressure along root chord, in.
y	spanwise distance from root chord, in.
\bar{y}	distance from root chord to wing center of pressure, in.
α	angle of attack, deg

APPARATUS

Wind Tunnel

The investigation was conducted in the Ames 1- by 3-foot supersonic wind tunnel No. 1. This single-return, continuous operation, variable-pressure wind tunnel has a Mach number range of 1.2 to 2.5. The Mach number is changed by varying the contour of flexible plates which comprise the top and bottom walls of the tunnel.

Models

Semispan models consisting of three triangular wings and two rectangular wings were constructed of hardened steel. A sketch identifying the models and a tabulation of their dimensions are presented in figure 1. Two triangular wings (aspect ratios 2 and 4) and one rectangular wing (aspect ratio 2) incorporated thickened root sections faired to integral hinge shaft extensions, since such thickening is generally required for supersonic all-movable wings to maintain structural integrity between the comparatively thin wing and a large hinge shaft. In order to assess the aerodynamic penalty of thickening the root sections, two of these wings, one triangular and one rectangular both of aspect ratio 2, were duplicated in plan form but had unthickened root sections and were provided with integral mounting flanges at their root chords. All wing sections in vertical streamwise planes were modified biconvex with maximum thickness ratios of 5 percent at midchord and with 50-percent-blunt trailing edges. Tubing was soldered into milled grooves on one surface of the wings and orifice holes were drilled from the opposite surface to communicate with the tubes at locations listed in table I in terms of spanwise and chordwise positions, y/s and x/c .

The wings were mounted on a boundary-layer plate serving both as a flow reflection plane and as a means of placing the wings in a region free of the tunnel-wall boundary layer. The thickened root wings were supported by their hinge shafts which fitted through a bearing in the boundary-layer plate. A clearance gap of 0.005 to 0.009 inch was allowed between these models and the boundary-layer plate to permit free rotation. The unthickened root wings were mounted on a turntable in the boundary-layer plate.

TESTS AND PROCEDURE

Range of Test Variables

All models were tested at Mach numbers of 1.45 and 1.97. The angle-of-attack range varied, depending on the Mach number and model, due to model structural limitations and manometer-board capacity. The largest angle-of-attack range of 0° to 50° was possible with model W_1 at Mach number 1.97. The smallest angle-of-attack range of 0° to 15° was obtained for model W_3 at Mach number 1.45. In order to determine the effects of Reynolds number, the models were tested at $R = 0.26 \times 10^6$ per inch and 0.44×10^6 per inch with some additional data taken at $R = 0.62 \times 10^6$ per inch for model W_5 at Mach number 1.45.

Reduction of Data

The local pressures were reduced to the pressure coefficient P as shown by the following expression:

$$P = \frac{p - p_o}{q} = \frac{p - p_w}{q} + \frac{p_w - p_o}{q}$$

where the term $(p - p_w)/q$ is calculated directly from the test data and $(p_w - p_o)/q$ is obtained from a calibration of the wind-tunnel air stream. Calibration of the air stream indicated that the value of $(p_w - p_o)/q$ at $M = 1.45$ was essentially 0, but that at $M = 1.97$ it was approximately 0.02.

Chordwise pressure distributions were integrated for each span station by a tabular method to give local span loading coefficient cc_n and local center of pressure \bar{x}/c . The absence of orifices at the leading and trailing edges of the wings required extrapolations of the pressure distribution to these points. Linear extrapolations were used, based, respectively, on the pressures measured at the first two and last two orifices of each span station. The spanwise load distributions were similarly integrated to give total load C_N and center-of-pressure location \bar{x}/c_r and \bar{y}/s . The span loadings beyond the most outboard station of the models were approximated by assuming a parabolic load distribution tangent to the slope passing through the loading of the last two outboard stations and falling to zero at the tip.

Validity of Data

In considering the validity of the data two questions arise - first, what is the measuring accuracy and second, how well does the semispan-model data represent the data for a full-span model? From an examination of the inaccuracy in setting the model angle of attack, the variations from constant test conditions, and the ability to repeat the pressure data in reruns at $R = 0.44 \times 10^6$ per inch, it was concluded that errors in measuring the pressure coefficients were less than ± 0.02 at both Mach numbers for the semispan wings tested. Although the second question cannot be answered so quantitatively, there is evidence in the case of the rectangular wings that with but few exceptions the measured pressures represent the pressures on a full-span wing. For the rectangular wing with unthickened root, the measured pressure distribution at span station $y/s = 0.025$, which was in close proximity to the juncture of the root chord and boundary-layer plate, was in good accord with values predicted by shock-expansion theory at both Mach numbers for angles of attack below shock detachment. At larger angles, if two-dimensional flow persisted at

the inboard span stations of the wing, then any spanwise deviation in pressure distribution in this region would be an indication of viscous effects due to the presence of the boundary-layer plate. Therefore, in absence of suitable theory, the pressure distribution of station $y/s = 0.025$ nearest the juncture of the root chord and boundary-layer plate was compared with that of the adjacent station ($y/s = 0.250$) at angles of attack slightly above that for shock detachment. No significant spanwise deviation in pressure distribution was found except between the pressures measured at the leading orifices of the two spanwise stations, indicating a localized interaction between the detached shock wave and plate boundary layer. This was the only evident boundary-layer interference effect on this rectangular wing and had negligible influence on the integrated forces and centers of pressure. The data for the thickened root rectangular wing could not be analyzed in the foregoing manner since the flow near the root chord was affected by the presence of the thickened root section. Since no large effects of Reynolds number at the most inboard span station were noted at $M = 1.45$, it was concluded that the plate boundary layer had little effect at this Mach number; however, at $M = 1.97$, more extensive indications of boundary-layer interference were evidenced, as will be pointed out in the discussion of Reynolds number effects. The effect of the gap between the wing and the boundary-layer plate on the wing loading was believed negligible on the basis of the findings of reference 4 in which it is shown that small gaps do not affect lift forces.

RESULTS

Tabulations of pressure coefficients are presented for the models at $M = 1.45$ and $M = 1.97$ for $R = 0.44 \times 10^6$ per inch in tables I(a) to I(j). The contributions to the loading and to center of pressure for each spanwise station are presented in tables II(a) to II(j) for both upper and lower wing surfaces. Summarized in tables II for each wing are also the normal-force coefficients, the center of pressure locations, and moment coefficients about the wing centroid of area. Figures 2 to 6 present plots of span loading coefficients, normal-force coefficients, and the center-of-pressure positions for each wing. Data taken at $R = 0.26 \times 10^6$ per inch and 0.62×10^6 per inch are also shown on these plots for comparison.

DISCUSSION

Angle-of-Attack Effects

All the wings showed a tendency toward uniform loading at high angles of attack in the range tested. This was indicated by the fact that with increasing angle of attack the span loading curves tended to assume the shape of the wing plan form, and the center-of-pressure position moved toward the wing centroid of area.

Effect of Thickened Root

The effect of thickening the root can be seen by comparing figures 2 and 5 for the aspect-ratio-2 triangular wings and figures 4 and 6 for the rectangular wings. At $M = 1.45$, the span loading did not seem to be greatly affected by the presence of the thickened root for either wing. The center-of-pressure position was little affected for the triangular wing; however, the center of pressure of the thickened root rectangular wing was about $0.01c_r$ forward of the center of pressure of the unthickened wing. At $M = 1.97$, for the angle-of-attack range below 17.5° (corresponding to shock detachment for the airfoil section), thickening the root section causes reductions in loading near the root chord such that the integrated normal-force coefficients were reduced by approximately 5 percent for both triangular and rectangular wings. At angles of attack above 17.5° , the difference in loading became smaller (1 to 2 percent) for both wings. Again, the center-of-pressure position was little affected for the triangular wing while the thickened root rectangular wing showed a forward shift of $0.01c_r$ in reference to that of the unthickened wing.

Effect of Reynolds Number

No large or systematic Reynolds number effects were noted except for the rectangular wing with thickened root at $M = 1.97$. For this case the pressure coefficients averaged 6 percent lower at $R = 0.26 \times 10^6$ per inch than the values at $R = 0.44 \times 10^6$ per inch over the angle-of-attack range tested. This difference was effective over the entire plan form and exceeded the possible error in measuring pressure coefficient throughout most of the angle-of-attack range. Pressure data for this wing tested on a larger boundary-layer plate at the same test conditions were compared with the present data in order to determine if this effect were due to the boundary layer on the plate. These results showed the same over-all Reynolds number effect but with slight variations at the most inboard station of the wing as compared with data taken on the smaller plate. It is surmised that the effect of Reynolds number was due to the combined effects of the thickened root and interaction between the strong leading-edge shock wave and the plate boundary layer.

Comparison with Force Data

As mentioned previously, the number of orifices were limited so chordwise and spanwise extrapolation of pressure distribution were required to obtain the integrated loads; hence, the accuracy of the

~~CONFIDENTIAL~~

integrated loads is open to some question. A check of the accuracy was obtained at $M = 1.97$ and $R = 0.44 \times 10^6$ per inch from direct measurement of the normal forces on the thickened root wings with a strain-gage balance. These measurements showed an agreement within experimental accuracy with those found from the integrated pressure results of the present test (figs. 2(b) to 4(b)).

CONCLUSIONS

Semispan pressure-distribution models of two triangular wings of aspect ratios 2 and 4 and one rectangular wing of aspect ratio 2, all with thickened root sections, and a triangular and rectangular wing, both of aspect ratio 2 without thickened root sections, were tested at $M = 1.45$ at angles of attack from 0° to 30° and at $M = 1.97$ at angles of attack from 0° to 50° . These tests support the following conclusions:

1. All the wings showed a tendency toward uniform loading at high angles of attack. Thus, with increasing angle of attack, the center of pressure moved toward the centroid of area, and the span loading curves tended to assume the shape of the wing plan form.

2. At $M = 1.45$, thickening the root section had little effect on the span loading for both the triangular and rectangular wings. At $M = 1.97$, for the angle-of-attack range below 17.5° , the presence of the thickened root tended to reduce the span loading near the root chord, resulting in a loss of approximately 5 percent in the integrated normal-force coefficients for both triangular and rectangular wings. The loss became smaller (1 to 2 percent) for angles of attack above 17.5° . The center-of-pressure position was little affected by the presence of a thickened root for the triangular wing but caused a slight forward shift (about 1 percent of the chord) in the case of the rectangular wing.

3. At $M = 1.97$, a decreased normal-force coefficient (6 percent) was noted for the thickened root rectangular wing at the lower Reynolds number of 0.26×10^6 per inch as compared with the values at $R = 0.44 \times 10^6$ per inch. This was the only case in which an appreciable or systematic effect of Reynolds number on normal-force coefficients occurred. The center-of-pressure position was negligibly affected for all wings in the range of Reynolds numbers at which the tests were conducted.

Ames Aeronautical Laboratory
National Advisory Committee for Aeronautics
Moffett Field, Calif., Apr. 19, 1954

REFERENCES

1. Moskowitz, Barry, and Maslen, Stephen H.: Experimental Pressure Distributions over Two Wing-Body Combinations at Mach Number 1.9. NACA RM E50J09, 1951.
2. Berler, Irving, and Nichols, Sidney: Interference Between Wing and Body at Supersonic Speeds. Part VI, Data Report. Pressure Distribution Tests of Wing-Body Interference Models at Mach No. of 2.0. Phase II, Tests of June, 1949. Cornell Aeronautical Lab., Inc., Buffalo. CAL/CF-1569, 1951.
3. Pitts, William C., Nielsen, Jack N., and Gionfriddo, Maurice P.: Comparison between Theory and Experiment for Interference Pressure Fields Between Wing and Body at Supersonic Speeds. NACA TN 3128, 1954.
4. Drake, William C.: Lift, Drag, and Hinge Moments at Supersonic Speeds of an All-Movable Triangular Wing and Body Combination. NACA RM A53F22, 1953.

~~CONFIDENTIAL~~

TABLE I.- PRESSURE COEFFICIENTS OF WINGS

(a) Wing 1; $M=1.97$; $R=0.44 \times 10^8$ per inch

7/6	5/6	Upper surface												Lower surface																																																																																																																																																																																																																																																																																																																																																																																																																																																																																																																																																																																																																																																																																																																																																																																																																																																																																																																																																																																																																																																																																																																																																						
		50°	47.5°	45°	42.5°	40°	37.5°	35°	32.5°	30°	27.5°	25°	22.5°	20°	17.5°	15°	12.5°	10°	7.5°	5°	2.5°	0°	2.5°	5°	7.5°	10°	12.5°	15°	17.5°	20°	22.5°	25°	27.5°	30°	32.5°	35°	37.5°	40°	42.5°	45°	47.5°	50°																																																																																																																																																																																																																																																																																																																																																																																																																																																																																																																																																																																																																																																																																																																																																																																																																																																																																																																																																																																																																																																																																																																										
0.000	0.003	-0.009	-0.031	-0.059	-0.087	-0.111	-0.136	-0.161	-0.186	-0.211	-0.236	-0.261	-0.286	-0.311	-0.336	-0.361	-0.386	-0.411	-0.436	-0.461	-0.486	-0.511	-0.536	-0.561	-0.586	-0.611	-0.636	-0.661	-0.686	-0.711	-0.736	-0.761	-0.786	-0.811	-0.836	-0.861	-0.886	-0.911	-0.936	-0.961	-0.986	-1.011	-1.036	-1.061	-1.086	-1.111	-1.136	-1.161	-1.186	-1.211	-1.236	-1.261	-1.286	-1.311	-1.336	-1.361	-1.386	-1.411	-1.436	-1.461	-1.486	-1.511	-1.536	-1.561	-1.586	-1.611	-1.636	-1.661	-1.686	-1.711	-1.736	-1.761	-1.786	-1.811	-1.836	-1.861	-1.886	-1.911	-1.936	-1.961	-1.986	-2.011	-2.036	-2.061	-2.086	-2.111	-2.136	-2.161	-2.186	-2.211	-2.236	-2.261	-2.286	-2.311	-2.336	-2.361	-2.386	-2.411	-2.436	-2.461	-2.486	-2.511	-2.536	-2.561	-2.586	-2.611	-2.636	-2.661	-2.686	-2.711	-2.736	-2.761	-2.786	-2.811	-2.836	-2.861	-2.886	-2.911	-2.936	-2.961	-2.986	-3.011	-3.036	-3.061	-3.086	-3.111	-3.136	-3.161	-3.186	-3.211	-3.236	-3.261	-3.286	-3.311	-3.336	-3.361	-3.386	-3.411	-3.436	-3.461	-3.486	-3.511	-3.536	-3.561	-3.586	-3.611	-3.636	-3.661	-3.686	-3.711	-3.736	-3.761	-3.786	-3.811	-3.836	-3.861	-3.886	-3.911	-3.936	-3.961	-3.986	-4.011	-4.036	-4.061	-4.086	-4.111	-4.136	-4.161	-4.186	-4.211	-4.236	-4.261	-4.286	-4.311	-4.336	-4.361	-4.386	-4.411	-4.436	-4.461	-4.486	-4.511	-4.536	-4.561	-4.586	-4.611	-4.636	-4.661	-4.686	-4.711	-4.736	-4.761	-4.786	-4.811	-4.836	-4.861	-4.886	-4.911	-4.936	-4.961	-4.986	-5.011	-5.036	-5.061	-5.086	-5.111	-5.136	-5.161	-5.186	-5.211	-5.236	-5.261	-5.286	-5.311	-5.336	-5.361	-5.386	-5.411	-5.436	-5.461	-5.486	-5.511	-5.536	-5.561	-5.586	-5.611	-5.636	-5.661	-5.686	-5.711	-5.736	-5.761	-5.786	-5.811	-5.836	-5.861	-5.886	-5.911	-5.936	-5.961	-5.986	-6.011	-6.036	-6.061	-6.086	-6.111	-6.136	-6.161	-6.186	-6.211	-6.236	-6.261	-6.286	-6.311	-6.336	-6.361	-6.386	-6.411	-6.436	-6.461	-6.486	-6.511	-6.536	-6.561	-6.586	-6.611	-6.636	-6.661	-6.686	-6.711	-6.736	-6.761	-6.786	-6.811	-6.836	-6.861	-6.886	-6.911	-6.936	-6.961	-6.986	-7.011	-7.036	-7.061	-7.086	-7.111	-7.136	-7.161	-7.186	-7.211	-7.236	-7.261	-7.286	-7.311	-7.336	-7.361	-7.386	-7.411	-7.436	-7.461	-7.486	-7.511	-7.536	-7.561	-7.586	-7.611	-7.636	-7.661	-7.686	-7.711	-7.736	-7.761	-7.786	-7.811	-7.836	-7.861	-7.886	-7.911	-7.936	-7.961	-7.986	-8.011	-8.036	-8.061	-8.086	-8.111	-8.136	-8.161	-8.186	-8.211	-8.236	-8.261	-8.286	-8.311	-8.336	-8.361	-8.386	-8.411	-8.436	-8.461	-8.486	-8.511	-8.536	-8.561	-8.586	-8.611	-8.636	-8.661	-8.686	-8.711	-8.736	-8.761	-8.786	-8.811	-8.836	-8.861	-8.886	-8.911	-8.936	-8.961	-8.986	-9.011	-9.036	-9.061	-9.086	-9.111	-9.136	-9.161	-9.186	-9.211	-9.236	-9.261	-9.286	-9.311	-9.336	-9.361	-9.386	-9.411	-9.436	-9.461	-9.486	-9.511	-9.536	-9.561	-9.586	-9.611	-9.636	-9.661	-9.686	-9.711	-9.736	-9.761	-9.786	-9.811	-9.836	-9.861	-9.886	-9.911	-9.936	-9.961	-9.986	-10.011	-10.036	-10.061	-10.086	-10.111	-10.136	-10.161	-10.186	-10.211	-10.236	-10.261	-10.286	-10.311	-10.336	-10.361	-10.386	-10.411	-10.436	-10.461	-10.486	-10.511	-10.536	-10.561	-10.586	-10.611	-10.636	-10.661	-10.686	-10.711	-10.736	-10.761	-10.786	-10.811	-10.836	-10.861	-10.886	-10.911	-10.936	-10.961	-10.986	-11.011	-11.036	-11.061	-11.086	-11.111	-11.136	-11.161	-11.186	-11.211	-11.236	-11.261	-11.286	-11.311	-11.336	-11.361	-11.386	-11.411	-11.436	-11.461	-11.486	-11.511	-11.536	-11.561	-11.586	-11.611	-11.636	-11.661	-11.686	-11.711	-11.736	-11.761	-11.786	-11.811	-11.836	-11.861	-11.886	-11.911	-11.936	-11.961	-11.986	-12.011	-12.036	-12.061	-12.086	-12.111	-12.136	-12.161	-12.186	-12.211	-12.236	-12.261	-12.286	-12.311	-12.336	-12.361	-12.386	-12.411	-12.436	-12.461	-12.486	-12.511	-12.536	-12.561	-12.586	-12.611	-12.636	-12.661	-12.686	-12.711	-12.736	-12.761	-12.786	-12.811	-12.836	-12.861	-12.886	-12.911	-12.936	-12.961	-12.986	-13.011	-13.036	-13.061	-13.086	-13.111	-13.136	-13.161	-13.186	-13.211	-13.236	-13.261	-13.286	-13.311	-13.336	-13.361	-13.386	-13.411	-13.436	-13.461	-13.486	-13.511	-13.536	-13.561	-13.586	-13.611	-13.636	-13.661	-13.686	-13.711	-13.736	-13.761	-13.786	-13.811	-13.836	-13.861	-13.886	-13.911	-13.936	-13.961	-13.986	-14.011	-14.036	-14.061	-14.086	-14.111	-14.136	-14.161	-14.186	-14.211	-14.236	-14.261	-14.286	-14.311	-14.336	-14.361	-14.386	-14.411	-14.436	-14.461	-14.486	-14.511	-14.536	-14.561	-14.586	-14.611	-14.636	-14.661	-14.686	-14.711	-14.736	-14.761	-14.786	-14.811	-14.836	-14.861	-14.886	-14.911	-14.936	-14.961	-14.986	-15.011	-15.036	-15.061	-15.086	-15.111	-15.136	-15.161	-15.186	-15.211	-15.236	-15.261	-15.286	-15.311	-15.336	-15.361	-15.386	-15.411	-15.436	-15.461	-15.486	-15.511	-15.536	-15.561	-15.586	-15.611	-15.636	-15.661	-15.686	-15.711	-15.736	-15.761	-15.786	-15.811	-15.836	-15.861	-15.886	-15.911	-15.936	-15.961	-15.986	-16.011	-16.036	-16.061	-16.086	-16.111	-16.136	-16.161	-16.186	-16.211	-16.236	-16.261	-16.286	-16.311	-16.336	-16.361	-16.386	-16.411	-16.436	-16.461	-16.486	-16.511	-16.536	-16.561	-16.586	-16.611	-16.636	-16.661	-16.686	-16.711	-16.736	-16.761	-16.786	-16.811	-16.836	-16.861	-16.886	-16.911	-16.936	-16.961	-16.986	-17.011	-17.036	-17.061	-17.086	-17.111	-17.136	-17.161	-17.186	-17.211	-17.236	-17.261	-17.286	-17.311	-17.336	-17.361	-17.386	-17.411	-17.436	-17.461	-17.486	-17.511	-17.536	-17.561	-17.586	-17.611	-17.636	-17.661	-17.686	-17.711	-17.736	-17.761	-17.786	-17.811	-17.836	-17.861	-17.886	-17.911	-17.936	-17.961	-17.986	-18.011	-18.036	-18.061	-18.086	-18.111	-18.136	-18.161	-18.186	-18.211	-18.236	-18.261	-18.286	-18.311	-18.336	-18.361	-18.386	-18.411	-18.436	-18.461	-18.486	-18.511	-18.536	-18.561	-18.586	-18.611	-18.636	-18.661	-18.686	-18.711	-18.736	-18.761	-18.786	-18.811	-18.836	-18.861	-18.886	-18.911	-18.936	-18.961	-18.986	-19.011	-19.036	-19.061	-19.086	-19.111	-19.136	-19.161	-19.186	-19.211	-19.236	-19.261	-19.286	-19.311	-19.336	-19.361	-19.386	-19.411	-19.436	-19.461	-19.486	-19.511	-19.536	-19.561	-19.586	-19.611	-19.636	-19.661	-19.686	-19.711	-19.736	-19.761	-19.786	-19.811	-19.836	-19.861	-19.886	-19.911	-19.936	-19.961	-19.986	-20.011	-20.036	-20.061	-20.086	-20.111	-20.136	-20.161	-20.186	-20.211	-20.236	-20.261	-20.286	-20.311	-20.336	-20.361	-20.386	-20.411	-20.436	-20.461	-20.486	-20.511	-20.536	-20.561	-20.586	-20.611	-20.636	-20.661	-20.686	-20.711	-20.736	-20.761	-20.786	-20.811	-20.836	-20.861	-20.886	-20.911	-20.936	-20.961	-20.986	-21.011	-21.036	-21.061	-21.086	-21.111	-21.136	-21.161	-21.186	-21.211	-21.236	-21.261	-21.286	-21.311	-21.336	-21.361	-21.386	-21.411	-21.436	-21.461	-21.486	-21.511	-21.536	-21.561	-21.586	-21.611	-21.636	-21.661	-21.686	-21.711	-21.736	-21.761	-21.786	-21.811	-21.836	-21.861	-21.886	-21.911	-21.936	-21.961	-21.986	-22.011	-22.036	-22.061	-22.086	-22.111	-22.136	-22.161	-22.186	-22.211	-22.236	-22.261	-22.286	-22.311	-22.336	-22.361	-22.386	-22.411	-22.436	-22.461	-22.486	-22.511	-22.536	-22.561	-22.586	-22.611	-22.636	-22.661	-22.686	-22.711	-22.736	-22.761	-22.786	-22.811	-22.836	-22.861	-22.886	-22.911	-22.936	-22.961	-22.986	-23.011	-23.036	-23.061	-23.086	-23.111	-23.136	-23.161	-23.186	-23.211	-23.236	-23.261	-23.286	-23.311	-23.336	-23.361	-23.386	-23.411	-23.436	-23.461	-23.486	-23.511	-23.536	-23.561	-23.586	-23.611	-23.636	-23.661	-23.686	-23.711	-23.736	-23.761	-23.786	-23.811	-23.836	-23.861	-23.886	-23.911	-23.936	-23.961	-23.986	-24.011	-24.036	-24.061	-24.086	-24.111	-24.136	-24.161	-24.186	-24.211	-24.236	-24.261	-24.286	-24.311	-24.336	-24.361	-24.386	-24.411	-24.436	-24.461	-24.486	-24.511	-24.536	-24.561	-24.586	-24.611	-24.636	-24.661	-24.686	-24.711	-24.736	-24.761	-24.786	-24.811	-24.836	-24.861	-24.886	-24.911	-24.936	-24.961	-24.986	-25.011	-25.036	-25.061	-25.086	-25.111	-25.136	-25.161	-25.186	-25.211	-25.236	-25.261	-25.286	-25.311	-25.336	-25.361	-25.386	-25.411	-25.436	-25.461	-25.486	-25.511	-25.536	-25.561	-25.586	-25.611	-25.636	-25.661	-25.686	-25.711	-25.736	-25.761	-25.786	-25.811	-25.836	-25.861	-25.886	-25.911	-25.936	-25.961	-25.986	-26.011	-26.036	-26.061	-26.086	-26.111	-26.136	-26.161	-26.186	-26.211	-26.236	-26.261	-26.286	-26.311	-26.336	-26.361	-26.386	-26.411	-26.436	-26.461	-26.486	-26.511	-26.536	-26.561	-26.586	-26.611	-26.636	-26.661	-26.686	-26.711	-26.736	-26.761	-26.786	-26.811	-26.836	-26.861	-26.886	-26.911	-26.936	-26.961	-26.986	-27.011	-27.036	-27.061	-27.086	-27.111	-27.136	-27.161	-27.186	-27.211	-27.236	-27.261	-27.286	-27.311	-27.336	-27.361	-27.386	-27.411	-27.436	-27.461	-27.486	-27.511	-27.536	-27.561	-27.586	-27.611	-27.636	-27.661	-27.686	-27.711	-27.736	-27.761	-27.786	-27.811	-27.836	-27.861	-27.886	-27.911	-27.936	-27.961	-27.986	-28.011	-28.036	-28.

(d) Wing 2; $M=1.97$; $R=0.44 \times 10^8$ per inch

		Upper surface												Lower surface											
74°	76°	78°	80°	82°	84°	86°	88°	90°	92°	94°	96°	98°	100°	102°	104°	106°	108°	110°	112°	114°	116°	118°	120°		
0.089	0.103	0.117	0.131	0.145	0.159	0.173	0.187	0.201	0.215	0.229	0.243	0.257	0.271	0.285	0.299	0.313	0.327	0.341	0.355	0.369	0.383	0.397	0.411	0.425	
	0.103	0.117	0.131	0.145	0.159	0.173	0.187	0.201	0.215	0.229	0.243	0.257	0.271	0.285	0.299	0.313	0.327	0.341	0.355	0.369	0.383	0.397	0.411	0.425	
	0.117	0.131	0.145	0.159	0.173	0.187	0.201	0.215	0.229	0.243	0.257	0.271	0.285	0.299	0.313	0.327	0.341	0.355	0.369	0.383	0.397	0.411	0.425	0.439	
	0.131	0.145	0.159	0.173	0.187	0.201	0.215	0.229	0.243	0.257	0.271	0.285	0.299	0.313	0.327	0.341	0.355	0.369	0.383	0.397	0.411	0.425	0.439	0.453	
	0.145	0.159	0.173	0.187	0.201	0.215	0.229	0.243	0.257	0.271	0.285	0.299	0.313	0.327	0.341	0.355	0.369	0.383	0.397	0.411	0.425	0.439	0.453	0.467	
	0.159	0.173	0.187	0.201	0.215	0.229	0.243	0.257	0.271	0.285	0.299	0.313	0.327	0.341	0.355	0.369	0.383	0.397	0.411	0.425	0.439	0.453	0.467	0.481	
	0.173	0.187	0.201	0.215	0.229	0.243	0.257	0.271	0.285	0.299	0.313	0.327	0.341	0.355	0.369	0.383	0.397	0.411	0.425	0.439	0.453	0.467	0.481	0.495	
	0.187	0.201	0.215	0.229	0.243	0.257	0.271	0.285	0.299	0.313	0.327	0.341	0.355	0.369	0.383	0.397	0.411	0.425	0.439	0.453	0.467	0.481	0.495	0.509	
	0.201	0.215	0.229	0.243	0.257	0.271	0.285	0.299	0.313	0.327	0.341	0.355	0.369	0.383	0.397	0.411	0.425	0.439	0.453	0.467	0.481	0.495	0.509	0.523	
	0.215	0.229	0.243	0.257	0.271	0.285	0.299	0.313	0.327	0.341	0.355	0.369	0.383	0.397	0.411	0.425	0.439	0.453	0.467	0.481	0.495	0.509	0.523	0.537	
	0.229	0.243	0.257	0.271	0.285	0.299	0.313	0.327	0.341	0.355	0.369	0.383	0.397	0.411	0.425	0.439	0.453	0.467	0.481	0.495	0.509	0.523	0.537	0.551	
	0.243	0.257	0.271	0.285	0.299	0.313	0.327	0.341	0.355	0.369	0.383	0.397	0.411	0.425	0.439	0.453	0.467	0.481	0.495	0.509	0.523	0.537	0.551	0.565	
	0.257	0.271	0.285	0.299	0.313	0.327	0.341	0.355	0.369	0.383	0.397	0.411	0.425	0.439	0.453	0.467	0.481	0.495	0.509	0.523	0.537	0.551	0.565	0.579	
	0.271	0.285	0.299	0.313	0.327	0.341	0.355	0.369	0.383	0.397	0.411	0.425	0.439	0.453	0.467	0.481	0.495	0.509	0.523	0.537	0.551	0.565	0.579	0.593	
0.500	0.515	0.529	0.543	0.557	0.571	0.585	0.599	0.613	0.627	0.641	0.655	0.669	0.683	0.697	0.711	0.725	0.739	0.753	0.767	0.781	0.795	0.809	0.823	0.837	
	0.515	0.529	0.543	0.557	0.571	0.585	0.599	0.613	0.627	0.641	0.655	0.669	0.683	0.697	0.711	0.725	0.739	0.753	0.767	0.781	0.795	0.809	0.823	0.837	
	0.529	0.543	0.557	0.571	0.585	0.599	0.613	0.627	0.641	0.655	0.669	0.683	0.697	0.711	0.725	0.739	0.753	0.767	0.781	0.795	0.809	0.823	0.837	0.851	
	0.543	0.557	0.571	0.585	0.599	0.613	0.627	0.641	0.655	0.669	0.683	0.697	0.711	0.725	0.739	0.753	0.767	0.781	0.795	0.809	0.823	0.837	0.851	0.865	
	0.557	0.571	0.585	0.599	0.613	0.627	0.641	0.655	0.669	0.683	0.697	0.711	0.725	0.739	0.753	0.767	0.781	0.795	0.809	0.823	0.837	0.851	0.865	0.879	
	0.571	0.585	0.599	0.613	0.627	0.641	0.655	0.669	0.683	0.697	0.711	0.725	0.739	0.753	0.767	0.781	0.795	0.809	0.823	0.837	0.851	0.865	0.879	0.893	
	0.585	0.599	0.613	0.627	0.641	0.655	0.669	0.683	0.697	0.711	0.725	0.739	0.753	0.767	0.781	0.795	0.809	0.823	0.837	0.851	0.865	0.879	0.893	0.907	
	0.599	0.613	0.627	0.641	0.655	0.669	0.683	0.697	0.711	0.725	0.739	0.753	0.767	0.781	0.795	0.809	0.823	0.837	0.851	0.865	0.879	0.893	0.907	0.921	
	0.613	0.627	0.641	0.655	0.669	0.683	0.697	0.711	0.725	0.739	0.753	0.767	0.781	0.795	0.809	0.823	0.837	0.851	0.865	0.879	0.893	0.907	0.921	0.935	
	0.627	0.641	0.655	0.669	0.683	0.697	0.711	0.725	0.739	0.753	0.767	0.781	0.795	0.809	0.823	0.837	0.851	0.865	0.879	0.893	0.907	0.921	0.935	0.949	
	0.641	0.655	0.669	0.683	0.697	0.711	0.725	0.739	0.753	0.767	0.781	0.795	0.809	0.823	0.837	0.851	0.865	0.879	0.893	0.907	0.921	0.935	0.949	0.963	
	0.655	0.669	0.683	0.697	0.711	0.725	0.739	0.753	0.767	0.781	0.795	0.809	0.823	0.837	0.851	0.865	0.879	0.893	0.907	0.921	0.935	0.949	0.963	0.977	
	0.669	0.683	0.697	0.711	0.725	0.739	0.753	0.767	0.781	0.795	0.809	0.823	0.837	0.851	0.865	0.879	0.893	0.907	0.921	0.935	0.949	0.963	0.977	0.991	
	0.683	0.697	0.711	0.725	0.739	0.753	0.767	0.781	0.795	0.809	0.823	0.837	0.851	0.865	0.879	0.893	0.907	0.921	0.935	0.949	0.963	0.977	0.991	1.005	
	0.697	0.711	0.725	0.739	0.753	0.767	0.781	0.795	0.809	0.823	0.837	0.851	0.865	0.879	0.893	0.907	0.921	0.935	0.949	0.963	0.977	0.991	1.005	1.019	
	0.711	0.725	0.739	0.753	0.767	0.781	0.795	0.809	0.823	0.837	0.851	0.865	0.879	0.893	0.907	0.921	0.935	0.949	0.963	0.977	0.991	1.005	1.019	1.033	
	0.725	0.739	0.753	0.767	0.781	0.795	0.809	0.823	0.837	0.851	0.865	0.879	0.893	0.907	0.921	0.935	0.949	0.963	0.977	0.991	1.005	1.019	1.033	1.047	
	0.739	0.753	0.767	0.781	0.795	0.809	0.823	0.837	0.851	0.865	0.879	0.893	0.907	0.921	0.935	0.949	0.963	0.977	0.991	1.005	1.019	1.033	1.047	1.061	
	0.753	0.767	0.781	0.795	0.809	0.823	0.837	0.851	0.865	0.879	0.893	0.907	0.921	0.935	0.949	0.963	0.977	0.991	1.005	1.019	1.033	1.047	1.061	1.075	
	0.767	0.781	0.795	0.809	0.823	0.837	0.851	0.865	0.879	0.893	0.907	0.921	0.935	0.949	0.963	0.977	0.991	1.005	1.019	1.033	1.047	1.061	1.075	1.089	
	0.781	0.795	0.809	0.823	0.837	0.851	0.865	0.879	0.893	0.907	0.921	0.935	0.949	0.963	0.977	0.991	1.005	1.019	1.033	1.047	1.061	1.075	1.089	1.103	
	0.795	0.809	0.823	0.837	0.851	0.865	0.879	0.893	0.907	0.921	0.935	0.949	0.963	0.977	0.991	1.005	1.019	1.033	1.047	1.061	1.075	1.089	1.103	1.117	
	0.809	0.823	0.837	0.851	0.865	0.879	0.893	0.907	0.921	0.935	0.949	0.963	0.977	0.991	1.005	1.019	1.033	1.047	1.061	1.075	1.089	1.103	1.117	1.131	
	0.823	0.837	0.851	0.865	0.879	0.893	0.907	0.921	0.935	0.949	0.963	0.977	0.991	1.005	1.019	1.033	1.047	1.061	1.075	1.089	1.103	1.117	1.131	1.145	
	0.837	0.851	0.865	0.879	0.893	0.907	0.921	0.935	0.949	0.963	0.977	0.991	1.005	1.019	1.033	1.047	1.061	1.075	1.089	1.103	1.117	1.131	1.145	1.159	
	0.851	0.865	0.879	0.893	0.907	0.921	0.935	0.949	0.963	0.977	0.991	1.005	1.019	1.033	1.047	1.061	1.075	1.089	1.103	1.117	1.131	1.145	1.159	1.173	
	0.865	0.879	0.893	0.907	0.921	0.935	0.949	0.963	0.977	0.991	1.005	1.019	1.033	1.047	1.061	1.075	1.089	1.103	1.117	1.131	1.145	1.159	1.173	1.187	
	0.879	0.893	0.907	0.921	0.935	0.949	0.963	0.977	0.991	1.005	1.019	1.033	1.047	1.061	1.075	1.089	1.103	1.117	1.131	1.145	1.159	1.173	1.187	1.201	
	0.893	0.907	0.921	0.935	0.949	0.963	0.977	0.991	1.005	1.019	1.033	1.047	1.061	1.075	1.089	1.103	1.117	1.131	1.145	1.159	1.173	1.187	1.201	1.215	
	0.907	0.921	0.935	0.949	0.963	0.977	0.991	1.005	1.019	1.033	1.047	1.061	1.075	1.089	1.103	1.117	1.131	1.145	1.159	1.173	1.187	1.201	1.215	1.229	
	0.921	0.935	0.949	0.963	0.977	0.991	1.005	1.019	1.033	1.047	1.061	1.075	1.089	1.103	1.117	1.131	1.145	1.159	1.173	1.187	1.201	1.215	1.229	1.243	
	0.935	0.949	0.963	0.977	0.991	1.005	1.019	1.033	1.047	1.061	1.075	1.089	1.103	1.117	1.131	1.145	1.159	1.173	1.187	1.201	1.215	1.229	1.243	1.257	
	0.949	0.963	0.977	0.991	1.005	1.019	1.033	1.047	1.061	1.075	1.089	1.103	1.117	1.131	1.145	1.159	1.173	1.187	1.201	1.215	1.229	1.243	1.257	1.271	
	0.963	0.977	0.991	1.005	1.019	1.033	1.047	1.061	1.075	1.089	1.103	1.117	1.131	1.145	1.159	1.173	1.187	1.201	1.215	1.229	1.243	1.257	1.271	1.285	
	0.977	0.991	1.005	1.019	1.033	1.047	1.061	1.075	1.089	1.103	1.117	1.131	1.145	1.159	1.173	1.187	1.201	1.215	1.229	1.243	1.257	1.271			



TABLE I.- PRESSURE COEFFICIENTS OF WINGS - Continued

(a) Wing 3; $M=1.45$; $R=0.44 \times 10^6$ per inch

(b) Wing 3; $M=1.97$; $R=0.44 \times 10^6$ per inch

(c) Wing 4; $M=1.45$; $R=0.44 \times 10^6$ per inch

(d) Wing 4; $M=1.97$; $R=0.44 \times 10^6$ per inch

The figure contains four sets of airfoil data tables, labeled (a) through (d). Each set corresponds to a specific wing configuration and flow condition. The tables are organized into two main sections: 'Upper surface' and 'Lower surface'. Each section contains a table of data points for various angles of attack (α) and Reynolds numbers (R). The data points are presented in a grid format, with the first column representing the angle of attack and the subsequent columns representing the Reynolds number. The data points are arranged in a way that allows for comparison between different wing configurations and flow conditions.

TABLE I.- PRESSURE COEFFICIENTS OF WINGS - Concluded

(i) Wing 5; M=1.45; R=0.44x10⁶ per inch

y/a	z/c	Upper surface							Lower surface						
		15.3°	12.8°	10.3°	7.8°	5.3°	2.8°	0.3°	3°	6°	10°	12.5°	15°	17.5°	
0.005	0.054	-0.316	-0.249	-0.163	-0.086	0.041	0.140	0.170	0.287	0.434	0.688	0.834	0.996	1.197	
	.141	-.291	-.256	-.207	-.127	0	.104	.136	.261	.434	.683	.814	.983	1.012	
	.242	-.331	-.275	-.216	-.148	-.058	.070	.102	.219	.369	.546	.645	.734	.814	
	.367	-.391	-.344	-.284	-.213	-.128	-.042	-.017	.080	.149	.245	.314	.368	.429	
	.492	-.393	-.348	-.288	-.216	-.131	-.046	-.021	.097	.165	.261	.330	.384	.445	
	.617	-.393	-.348	-.288	-.216	-.131	-.046	-.021	.097	.165	.261	.330	.384	.445	
	.805	-.393	-.348	-.288	-.216	-.131	-.046	-.021	.097	.165	.261	.330	.384	.445	
	.953	-.393	-.348	-.288	-.216	-.131	-.046	-.021	.097	.165	.261	.330	.384	.445	
.250	0.054	-.338	-.246	-.154	-.077	.053	.168	.204	.336	.483	.663	.853	1.042	1.114	
	.141	-.315	-.242	-.167	-.091	.028	.146	.189	.329	.476	.642	.827	.991	.974	
	.242	-.348	-.275	-.201	-.128	.037	.157	.207	.349	.493	.653	.833	.993	.974	
	.367	-.368	-.294	-.220	-.148	.046	.166	.216	.359	.503	.663	.843	.993	.974	
	.492	-.368	-.294	-.220	-.148	.046	.166	.216	.359	.503	.663	.843	.993	.974	
	.617	-.368	-.294	-.220	-.148	.046	.166	.216	.359	.503	.663	.843	.993	.974	
	.805	-.368	-.294	-.220	-.148	.046	.166	.216	.359	.503	.663	.843	.993	.974	
	.953	-.368	-.294	-.220	-.148	.046	.166	.216	.359	.503	.663	.843	.993	.974	
.563	0.054	-.393	-.271	-.189	-.096	.038	.198	.238	.390	.560	.818	.994	1.023	1.100	
	.141	-.365	-.258	-.181	-.118	.009	.221	.271	.423	.593	.844	.994	.994	.994	
	.242	-.343	-.266	-.189	-.125	.031	.232	.282	.434	.604	.855	.994	.994	.994	
	.367	-.368	-.294	-.220	-.148	.046	.233	.283	.435	.605	.856	.994	.994	.994	
	.492	-.368	-.294	-.220	-.148	.046	.233	.283	.435	.605	.856	.994	.994	.994	
	.617	-.368	-.294	-.220	-.148	.046	.233	.283	.435	.605	.856	.994	.994	.994	
	.805	-.368	-.294	-.220	-.148	.046	.233	.283	.435	.605	.856	.994	.994	.994	
	.953	-.368	-.294	-.220	-.148	.046	.233	.283	.435	.605	.856	.994	.994	.994	
.875	0.054	-.389	-.251	-.170	-.087	.054	.212	.252	.398	.575	.833	.994	.994	.994	
	.141	-.366	-.251	-.170	-.101	.002	.222	.272	.424	.594	.845	.994	.994	.994	
	.242	-.346	-.251	-.170	-.101	.002	.222	.272	.424	.594	.845	.994	.994	.994	
	.367	-.366	-.251	-.170	-.101	.002	.222	.272	.424	.594	.845	.994	.994	.994	
	.492	-.366	-.251	-.170	-.101	.002	.222	.272	.424	.594	.845	.994	.994	.994	
	.617	-.366	-.251	-.170	-.101	.002	.222	.272	.424	.594	.845	.994	.994	.994	
	.805	-.366	-.251	-.170	-.101	.002	.222	.272	.424	.594	.845	.994	.994	.994	
	.953	-.366	-.251	-.170	-.101	.002	.222	.272	.424	.594	.845	.994	.994	.994	

(j) Wing 5; M=1.97; R=0.44x10⁶ per inch

y/a	z/c	Upper surface							Lower surface						
		30°	25°	20°	15°	10°	6°	3°	0°	3°	6°	10°	15°	20°	30°
0.005	0.054	-0.285	-0.256	-0.208	-0.146	-0.065	0.008	0.069	0.138	0.216	0.301	0.431	0.640	0.985	1.342
	.141	-.243	-.236	-.214	-.163	-.094	-.006	.008	.082	.168	.272	.401	.640	.961	1.308
	.242	-.266	-.257	-.224	-.178	-.113	-.046	.012	.075	.150	.254	.370	.508	.839	1.077
	.367	-.266	-.257	-.224	-.178	-.113	-.046	.012	.075	.150	.254	.370	.508	.839	1.077
	.492	-.266	-.257	-.224	-.178	-.113	-.046	.012	.075	.150	.254	.370	.508	.839	1.077
	.617	-.266	-.257	-.224	-.178	-.113	-.046	.012	.075	.150	.254	.370	.508	.839	1.077
	.805	-.266	-.257	-.224	-.178	-.113	-.046	.012	.075	.150	.254	.370	.508	.839	1.077
	.953	-.266	-.257	-.224	-.178	-.113	-.046	.012	.075	.150	.254	.370	.508	.839	1.077
.250	0.054	-.298	-.251	-.188	-.119	-.080	-.006	.077	.126	.210	.300	.447	.689	1.060	1.308
	.141	-.262	-.253	-.215	-.166	-.099	-.005	.037	.106	.189	.276	.415	.644	.917	1.097
	.242	-.276	-.251	-.224	-.175	-.110	-.042	.015	.080	.157	.247	.380	.508	.795	1.084
	.367	-.293	-.269	-.237	-.194	-.130	-.067	.012	.047	.118	.196	.321	.447	.687	.866
	.492	-.300	-.289	-.253	-.211	-.139	-.094	.041	.019	.082	.157	.276	.447	.687	.866
	.617	-.296	-.289	-.253	-.211	-.139	-.094	.041	.019	.082	.157	.276	.447	.687	.866
	.805	-.296	-.289	-.253	-.211	-.139	-.094	.041	.019	.082	.157	.276	.447	.687	.866
	.953	-.296	-.289	-.253	-.211	-.139	-.094	.041	.019	.082	.157	.276	.447	.687	.866
.563	0.054	-.308	-.259	-.205	-.129	-.087	-.015	.047	.118	.201	.290	.436	.672	1.038	1.277
	.141	-.287	-.256	-.218	-.171	-.099	-.028	.033	.101	.180	.266	.407	.627	.922	1.235
	.242	-.289	-.264	-.231	-.189	-.120	-.054	.003	.068	.143	.227	.358	.560	.799	1.074
	.367	-.293	-.276	-.244	-.215	-.140	-.076	.023	.037	.108	.186	.318	.480	.642	.790
	.492	-.293	-.276	-.244	-.215	-.140	-.076	.023	.037	.108	.186	.318	.480	.642	.790
	.617	-.293	-.276	-.244	-.215	-.140	-.076	.023	.037	.108	.186	.318	.480	.642	.790
	.805	-.293	-.276	-.244	-.215	-.140	-.076	.023	.037	.108	.186	.318	.480	.642	.790
	.953	-.293	-.276	-.244	-.215	-.140	-.076	.023	.037	.108	.186	.318	.480	.642	.790
.875	0.054	-.280	-.238	-.205	-.125	-.080	-.004	.061	.132	.215	.306	.454	.682	.930	1.200
	.141	-.272	-.237	-.208	-.162	-.094	-.023	.030	.105	.185	.266	.404	.644	.912	1.122
	.242	-.270	-.213	-.201	-.153	-.088	-.033	.014	.068	.131	.185	.291	.429	.611	.798
	.367	-.244	-.221	-.175	-.136	-.094	-.047	.017	.039	.094	.118	.205	.335	.504	.674
	.492	-.266	-.240	-.197	-.149	-.098	-.067	.047	.010	.086	.070	.170	.270	.424	.573
	.617	-.266	-.240	-.197	-.149	-.098	-.067	.047	.010	.086	.070	.170	.270	.424	.573
	.805	-.266	-.240	-.197	-.149	-.098	-.067	.047	.010	.086	.070	.170	.270	.424	.573
	.953	-.266	-.240	-.197	-.149	-.098	-.067	.047	.010	.086	.070	.170	.270	.424	.573

NACA

TABLE II.- SPAN LOAD DISTRIBUTION, NORMAL FORCE, AND CENTER OF PRESSURE OF WING - Continued

14

(e) Wing 3; $M=1.46$; $R=0.44 \times 10^6$ per inch.

γ/a	C_n , section normal-force coefficient												\bar{x}/c , section center of pressure												Entire wing			
	Upper surface				Lower surface				Both surfaces				Upper surface				Lower surface				Both surfaces				C_x	C_n	\bar{x}/c	\bar{y}/s
	0.005	0.250	0.503	0.875	0.005	0.250	0.503	0.875	0.005	0.250	0.503	0.875	0.005	0.250	0.503	0.875	0.005	0.250	0.503	0.875	0.005	0.250	0.503	0.875				
30°	0.091	0.087	0.076	0.046	0.098	0.104	0.088	0.079	0.189	0.191	0.169	0.104	0.456	0.433	0.383	0.337	0.434	0.413	0.351	0.334	0.445	0.428	0.387	0.337	0.124	0.016	0.399	0.403
60°	.181	.167	.146	.096	.208	.213	.191	.187	.390	.380	.337	.282	.808	.744	.657	.579	.808	.744	.657	.579	.830	.744	.657	.579	.317	.035	.380	.433
100°	.266	.269	.237	.173	.338	.336	.306	.287	.684	.602	.544	.399	.869	.847	.703	.599	.869	.847	.703	.599	.831	.811	.680	.517	.094	.094	.396	.441
150°	.404	.395	.348	.278	.504	.485	.443	.378	.908	.871	.791	.635	.965	.942	.803	.697	.965	.942	.803	.697	.931	.911	.780	.614	.068	.068	.411	.448

(f) Wing 3; $M=1.07$; $R=0.44 \times 10^6$ per inch.

γ/a	C_n , section normal-force coefficient												\bar{x}/c , section center of pressure												Entire wing			
	Upper surface				Lower surface				Both surfaces				Upper surface				Lower surface				Both surfaces				C_x	C_n	\bar{x}/c	\bar{y}/s
	0.005	0.250	0.503	0.875	0.005	0.250	0.503	0.875	0.005	0.250	0.503	0.875	0.005	0.250	0.503	0.875	0.005	0.250	0.503	0.875	0.005	0.250	0.503	0.875				
30°	0.049	0.053	0.053	0.035	0.060	0.056	0.064	0.048	0.109	0.118	0.116	0.077	0.441	0.421	0.447	0.358	0.471	0.449	0.451	0.367	0.477	0.450	0.449	0.363	0.103	0.006	0.438	0.451
60°	.101	.105	.103	.070	.132	.128	.134	.093	.233	.243	.237	.163	.577	.550	.544	.378	.600	.566	.551	.376	.670	.648	.648	.374	.214	.013	.437	.449
100°	.159	.161	.158	.116	.147	.142	.148	.118	.406	.412	.400	.293	.683	.649	.643	.468	.701	.666	.654	.468	.772	.744	.744	.469	.369	.021	.448	.458
150°	.217	.215	.211	.177	.226	.217	.221	.183	.563	.531	.523	.362	.850	.822	.813	.577	.872	.836	.818	.566	.940	.912	.912	.569	.270	.034	.440	.456
200°	.263	.263	.249	.224	.284	.271	.271	.240	.696	.648	.641	.448	.948	.911	.904	.647	.969	.933	.919	.647	.989	.967	.967	.647	.277	.094	.430	.458
250°	.298	.284	.278	.252	.311	.297	.297	.266	.776	.715	.715	.481	.994	.957	.949	.682	.994	.957	.949	.682	.994	.969	.969	.682	.277	.097	.430	.460
300°	.315	.308	.303	.288	.359	.348	.348	.317	.820	.759	.759	.511	1.004	.967	.959	.703	1.004	.967	.959	.703	1.004	.979	.979	.703	.277	.097	.430	.460
350°	.326	.316	.311	.305	.369	.358	.358	.327	.849	.788	.788	.531	1.014	.977	.969	.723	1.014	.977	.969	.723	1.014	.989	.989	.723	.277	.097	.430	.460
400°	.330	.323	.318	.310	.370	.359	.359	.328	.859	.798	.798	.541	1.014	.977	.969	.733	1.014	.977	.969	.733	1.014	.989	.989	.733	.277	.097	.430	.460
450°	.333	.326	.321	.312	.373	.362	.362	.331	.869	.808	.808	.551	1.014	.977	.969	.743	1.014	.977	.969	.743	1.014	.989	.989	.743	.277	.097	.430	.460

(g) Wing 4; $M=1.45$; $R=0.44 \times 10^6$ per inch.

γ/a	C_n , section normal-force coefficient															\bar{x}/c , section center of pressure															Entire wing					
	Upper surface					Lower surface					Both surfaces					Upper surface					Lower surface					Both surfaces					C_x	C_n	\bar{x}/c	\bar{y}/s		
	0.005	0.250	0.500	0.750	0.875	0.005	0.250	0.500	0.750	0.875	0.005	0.250	0.500	0.750	0.875	0.005	0.250	0.500	0.750	0.875	0.005	0.250	0.500	0.750	0.875	0.005	0.250	0.500	0.750	0.875						
30°	0.039	0.038	0.086	0.149	0.160	0.047	0.048	0.054	0.108	0.086	0.100	0.146	0.433	0.409	0.388	0.368	0.433	0.409	0.388	0.368	0.433	0.409	0.388	0.368	0.433	0.409	0.388	0.368	0.433	0.409	0.388	0.368	0.433	0.409	0.388	0.368
60°	.078	.160	.127	.060	.073	.099	.108	.128	.177	.183	.177	.228	.309	.437	.476	.474	.373	.441	.360	.463	.473	.303	.465	.477	.400	.264	-.005	.681	0.418	0.304	.391	.404	.404	.404		
100°	.130	.169	.141	.095	.144	.178	.188	.206	.249	.280	.300	.377	.547	.680	.688	.474	.568	.460	.468	.563	.463	.443	.481	.486	.443	.478	.311	.669	.391	.391	.391	.391	.391	.391		
150°	.157	.269	.198	.146	.173	.244	.256	.278	.308	.345	.364	.404	.589	.730	.724	.566	.574	.477	.470	.568	.462	.479	.467	.501	.469	.471	.482	.481	.314	.482	.481	.314	.482	.481		
200°	.186	.336	.204	.145	.192	.284	.308	.313	.348	.387	.400	.436	.637	.799	.782	.581	.579	.469	.462	.563	.463	.469	.461	.504	.469	.462	.531	.489	.313	.489	.313	.489	.313	.489		
250°	.218	.409	.227	.173	.219	.339	.365	.371	.399	.444	.473	.513	.708	.863	.835	.598	.584	.469	.462	.563	.463	.469	.461	.504	.469	.462	.531	.489	.313	.489	.313	.489	.313	.489		

(h) Wing 4; $M=1.07$; $R=0.44 \times 10^6$ per inch.

γ/a °	C_n , section normal-force coefficient												\bar{x}/c , section center of pressure												Entire wing					
	Upper surface				Lower surface				Both surfaces				Upper surface				Lower surface				Both surfaces				C_x	C_m	\bar{x}/c_r	\bar{y}/s		
	0.005	0.250	0.500	0.750	0.875	0.005	0.250	0.500	0.750	0.875	0.025	0.250	0.500	0.750	0.875	0.025	0.250	0.500	0.750	0.875	0.025	0.250	0.500	0.750					0.875	
0	0.032	0.040	0.046	0.086	0.098	0.036	0.046	0.054	0.067	0.075	0.070	0.086	0.100	0.133	0.174	0.476	0.445	0.434	0.339	0.336	0.433	0.422	0.439	0.472	0.464	0.398	0.393	0.688	0.393	
30	.064	.077	.135	.211	.244	.092	.106	.123	.134	.145	.124	.169	.248	.334	.378	.403	.447	.349	.374	.440	.488	.464	.464	.472	.484	.466	.394	.430	.456	.464
60	.096	.148	.215	.298	.344	.120	.153	.180	.215	.245	.244	.311	.397	.494	.561	.603	.603	.489	.473	.569	.609	.579	.569	.569	.569	.430	.430	.456	.464	
90	.134	.228	.309	.396	.463	.163	.207	.246	.286	.324	.324	.389	.480	.569	.623	.683	.683	.569	.569	.623	.683	.683	.683	.683	.683	.430	.430	.456	.464	
120	.167	.271	.354	.437	.517	.200	.250	.300	.340	.384	.384	.454	.549	.639	.693	.714	.721	.603	.589	.639	.693	.693	.693	.693	.693	.430	.430	.456	.464	
150	.211	.319	.385	.463	.546	.248	.304	.354	.394	.438	.438	.508	.603	.693	.747	.768	.768	.603	.589	.639	.693	.693	.693	.693	.693	.430	.430	.456	.464	
180	.277	.389	.460	.537	.621	.300	.360	.410	.450	.494	.494	.564	.659	.749	.803	.824	.824	.659	.645	.693	.749	.749	.749	.749	.749	.430	.430	.456	.464	

NACA

TABLE II.- SPAN LOAD DISTRIBUTION, NORMAL FORCE, AND CENTER OF PRESSURE OF WING - Concluded

(1) Wing 5; $M=1.45$; $R=0.44 \times 10^6$ per inch

α °	C_n , section normal-force coefficient												\bar{x}/c , section center of pressure												Entire wing			
	Upper surface				Lower surface				Both surfaces				Upper surface				Lower surface				Both surfaces				C_N	C_m	\bar{x}/c_r	\bar{y}/s
	0.025	0.250	0.563	0.875	0.025	0.250	0.563	0.875	0.025	0.250	0.563	0.875	0.025	0.250	0.563	0.875	0.025	0.250	0.563	0.875	0.025	0.250	0.563	0.875				
3°	0.095	0.089	0.080	0.049	0.095	0.101	0.088	0.096	0.190	0.190	0.169	0.105	0.464	0.432	0.394	0.322	0.434	0.422	0.392	0.333	0.449	0.427	0.393	0.328	0.156	0.015	0.403	0.430
6°	.180	.172	.148	.100	.199	.215	.189	.121	.379	.387	.337	.221	.470	.442	.398	.366	.408	.389	.374	.338	.437	.413	.385	.351	.316	.033	.396	.433
10°	.284	.281	.242	.179	.330	.338	.308	.217	.614	.619	.550	.396	.473	.456	.404	.424	.401	.396	.380	.350	.434	.423	.391	.383	.320	.049	.405	.440
12.5°	.343	.342	.300	.237	.413	.411	.380	.284	.756	.753	.680	.520	.470	.454	.411	.442	.403	.406	.390	.363	.433	.428	.399	.399	.346	.057	.412	.446
15°	.399	.397	.351	.291	.491	.477	.446	.347	.889	.874	.797	.637	.471	.452	.412	.450	.407	.415	.400	.374	.436	.432	.405	.409	.766	.061	.421	.446
17.5°	.450	.449	.396	.335	.579	.547	.513	.410	1.029	.996	.909	.744	.472	.449	.413	.460	.408	.424	.410	.386	.436	.435	.411	.419	.874	.067	.423	.450

(2) Wing 5; $M=1.87$; $R=0.44 \times 10^6$ per inch

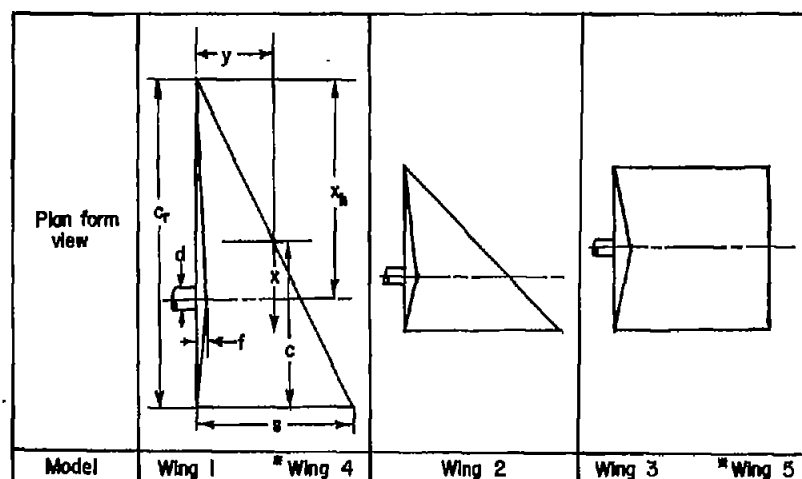
α °	C_n , section normal-force coefficient												\bar{x}/c , section center of pressure												Entire wing			
	Upper surface				Lower surface				Both surfaces				Upper surface				Lower surface				Both surfaces				C_N	C_m	\bar{x}/c_r	\bar{y}/s
	0.025	0.250	0.563	0.875	0.025	0.250	0.563	0.875	0.025	0.250	0.563	0.875	0.025	0.250	0.563	0.875	0.025	0.250	0.563	0.875	0.025	0.250	0.563	0.875				
3°	0.060	0.064	0.059	0.037	0.071	0.069	0.064	0.045	0.131	0.133	0.123	0.082	0.484	0.451	0.436	0.353	0.480	0.467	0.458	0.387	0.482	0.459	0.447	0.361	0.113	0.006	0.443	0.441
6°	.115	.113	.108	.073	.149	.148	.135	.096	.264	.261	.243	.169	.478	.471	.446	.377	.478	.446	.455	.384	.478	.457	.451	.381	.225	.012	.446	.442
10°	.178	.174	.167	.123	.274	.266	.246	.184	.452	.440	.413	.307	.477	.465	.448	.413	.479	.440	.447	.403	.478	.450	.447	.407	.386	.020	.447	.447
15°	.240	.232	.225	.186	.456	.441	.405	.318	.696	.673	.630	.504	.474	.464	.449	.442	.469	.453	.440	.415	.471	.457	.443	.425	.599	.031	.448	.451
20°	.283	.269	.264	.235	.653	.625	.583	.478	.936	.894	.847	.713	.471	.461	.452	.457	.444	.433	.426	.422	.452	.441	.434	.434	.808	.050	.438	.456
25°	.317	.307	.299	.272	.833	.771	.736	.639	1.150	1.078	1.035	.911	.469	.464	.452	.466	.438	.435	.428	.423	.447	.443	.435	.436	.992	.060	.440	.460
30°	.328	.325	.320	.300	1.000	.899	.870	.791	1.328	1.224	1.190	1.091	.467	.455	.446	.459	.450	.442	.435	.424	.454	.445	.438	.434	1.147	.067	.442	.463

NACA

~~CONFIDENTIAL~~

NACA RM A54D19

~~CONFIDENTIAL~~



*Wings having duplicate plan forms but mounted on turntable and without thickened root section

A	2	4	2
c_r in	8	4	4
s in	4	4	4
x_b/c_r	.667	.667	.500
S in ²	16	8	16
d in	.875	.625	.625
f in	.250	.350	.400

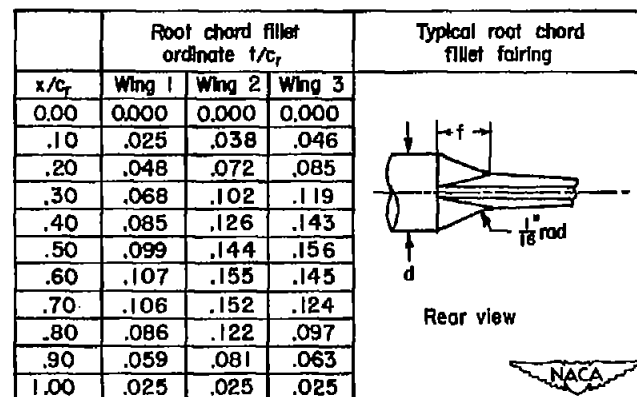
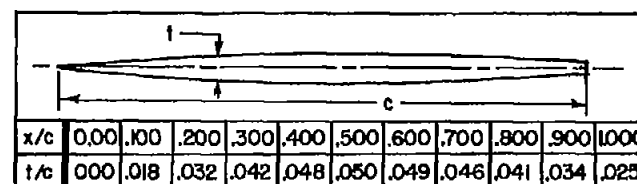
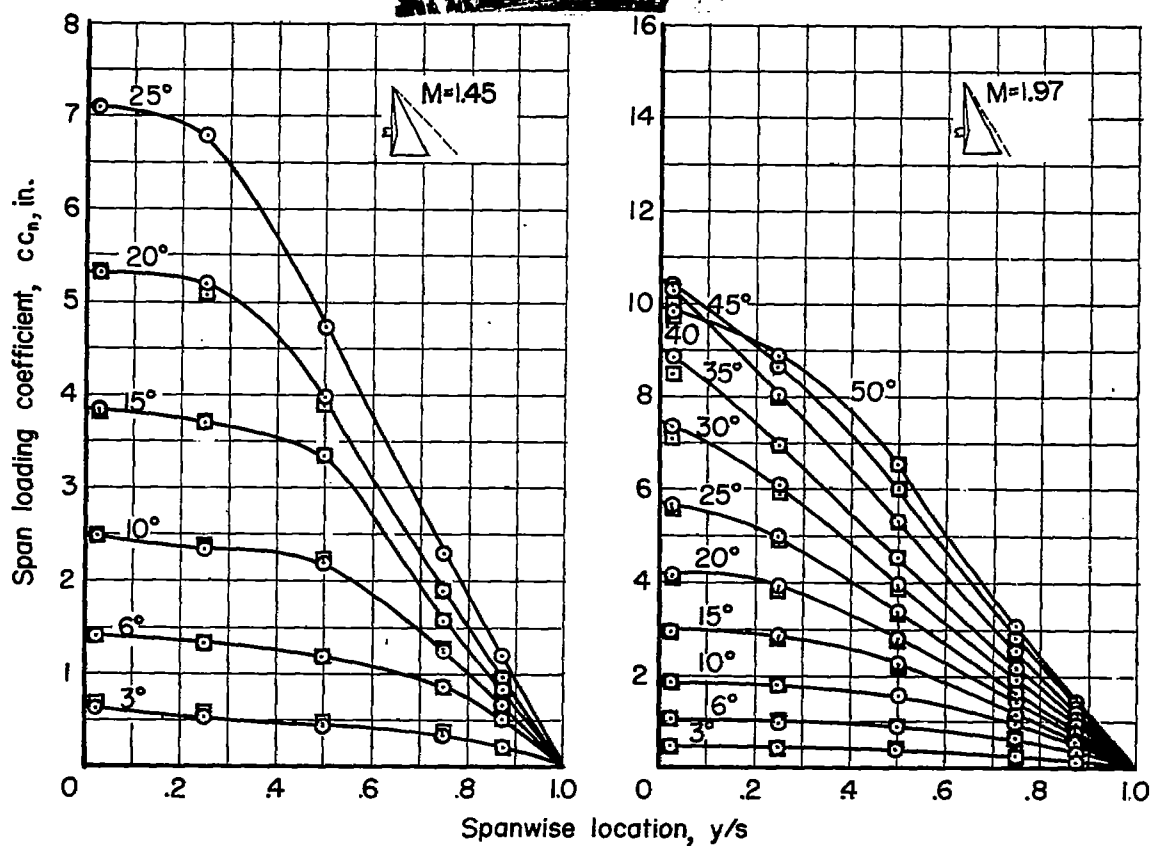
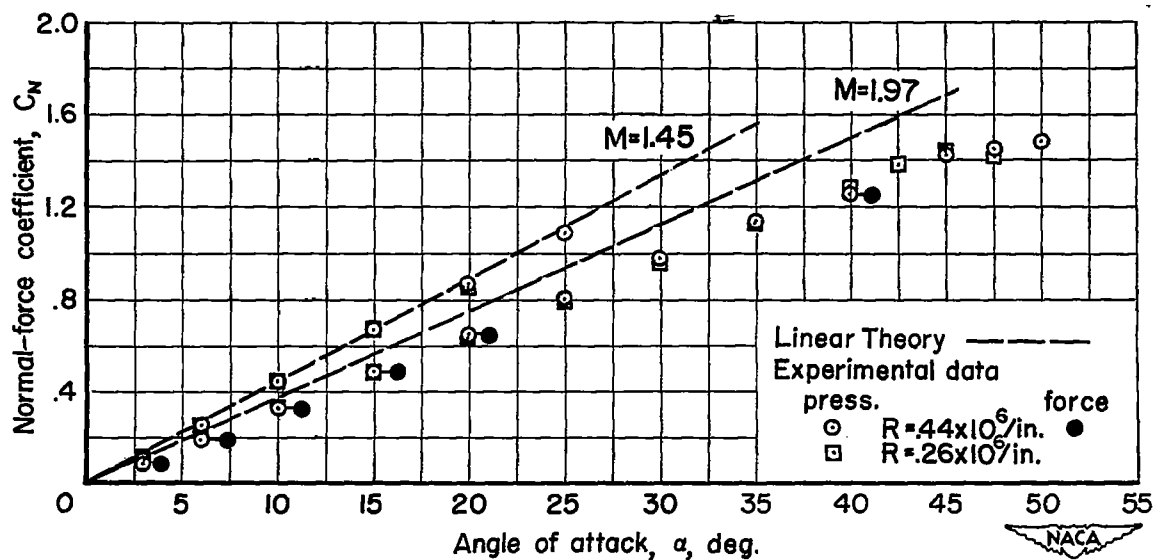


Figure 1.- Wing dimensions and identity.



(a) Span loading.



(b) Normal-force curves.

Figure 2.- Aerodynamic characteristics of wing 1.

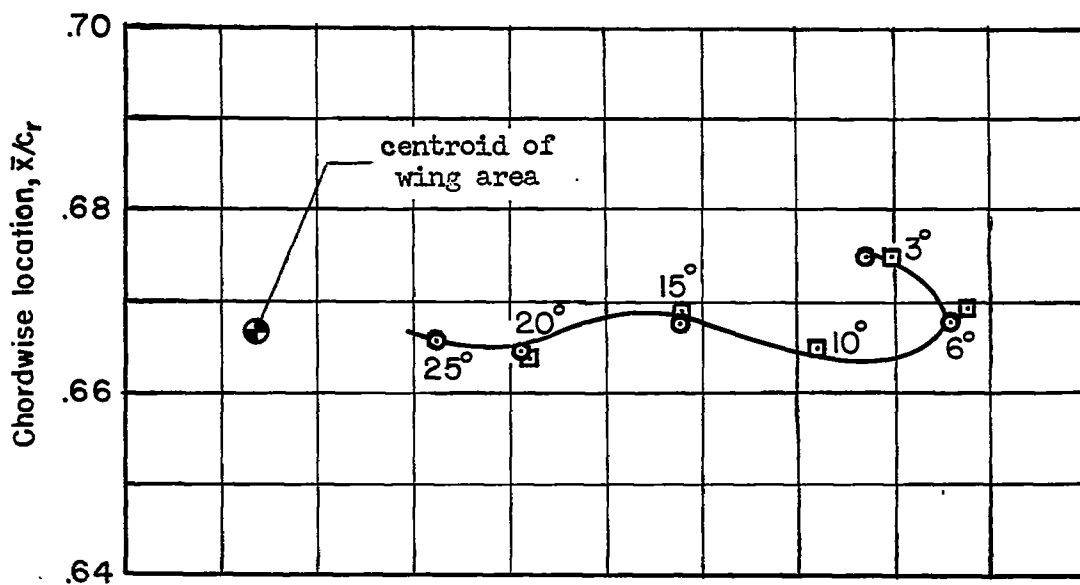
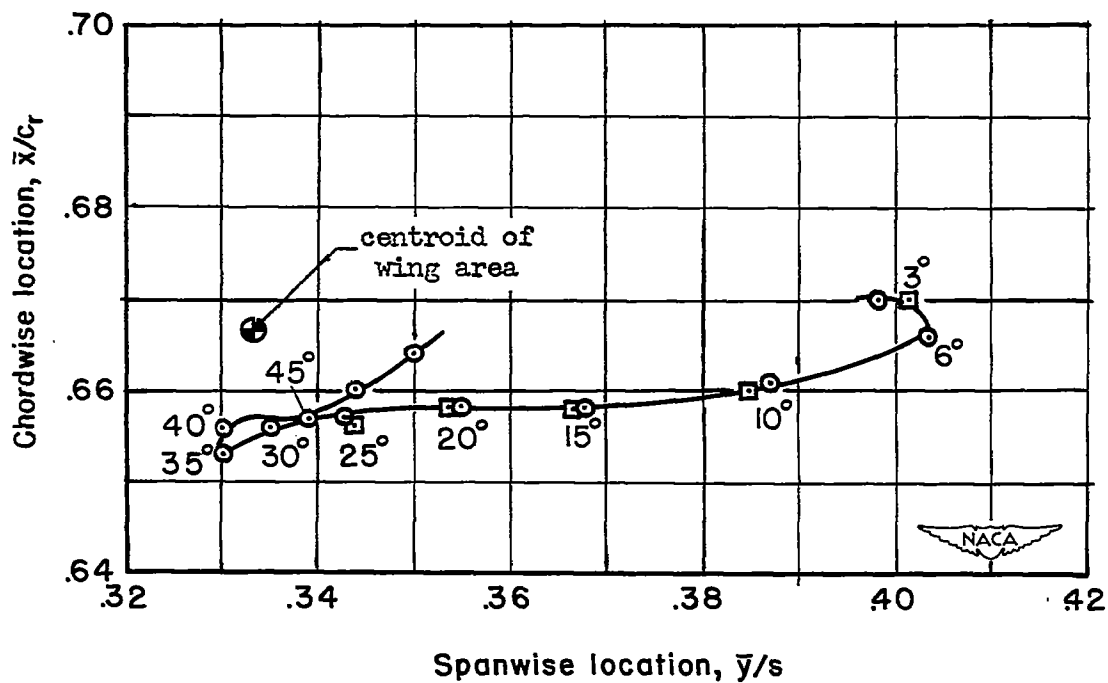
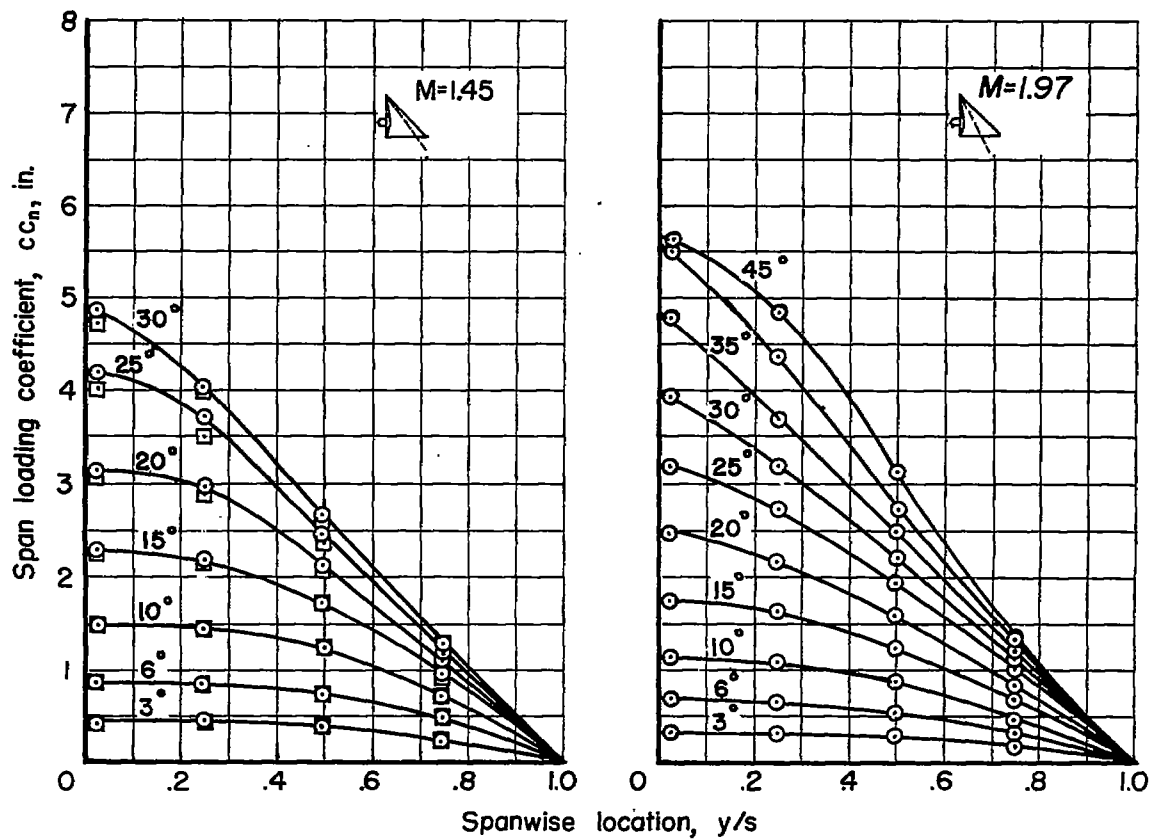
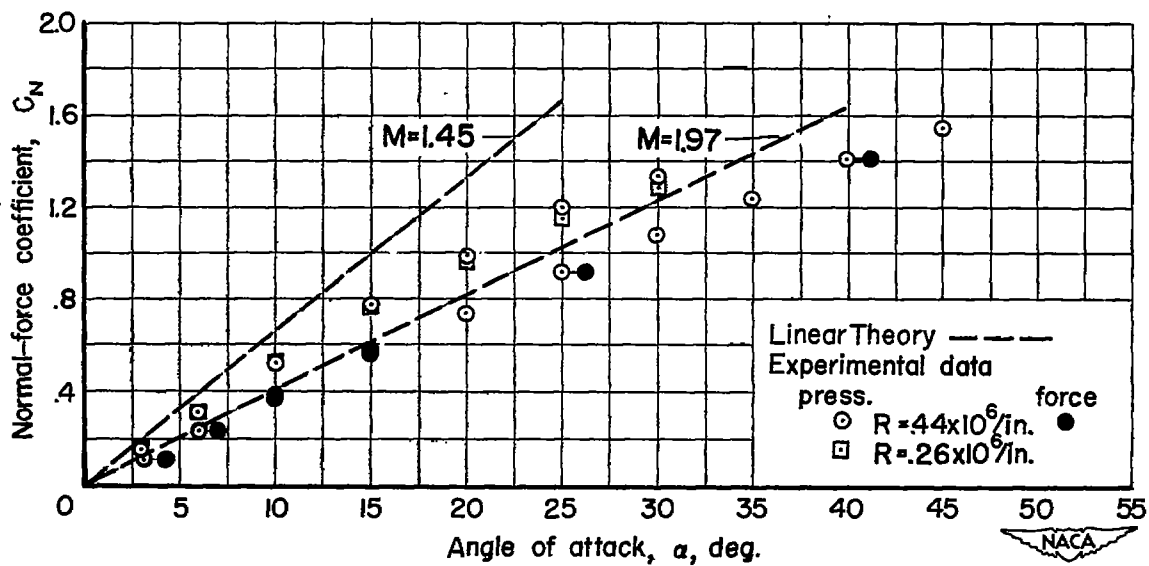
(c) Center-of-pressure position; $M = 1.45$.(d) Center-of-pressure position; $M = 1.97$.

Figure 2.- Concluded.



(a) Span loading.



(b) Normal force.

Figure 3.- Aerodynamic characteristics of wing 2.

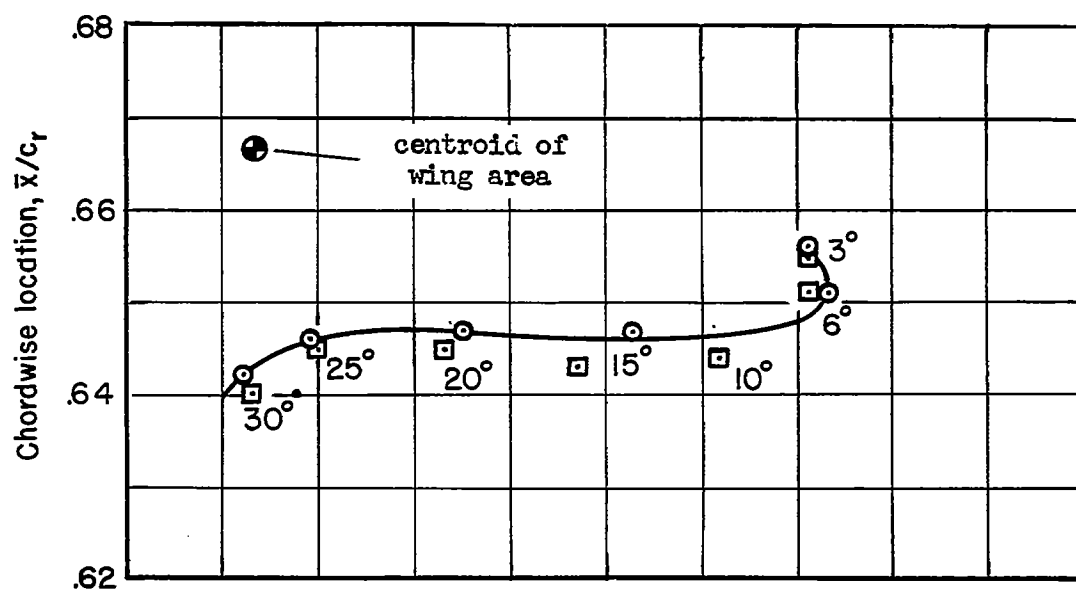
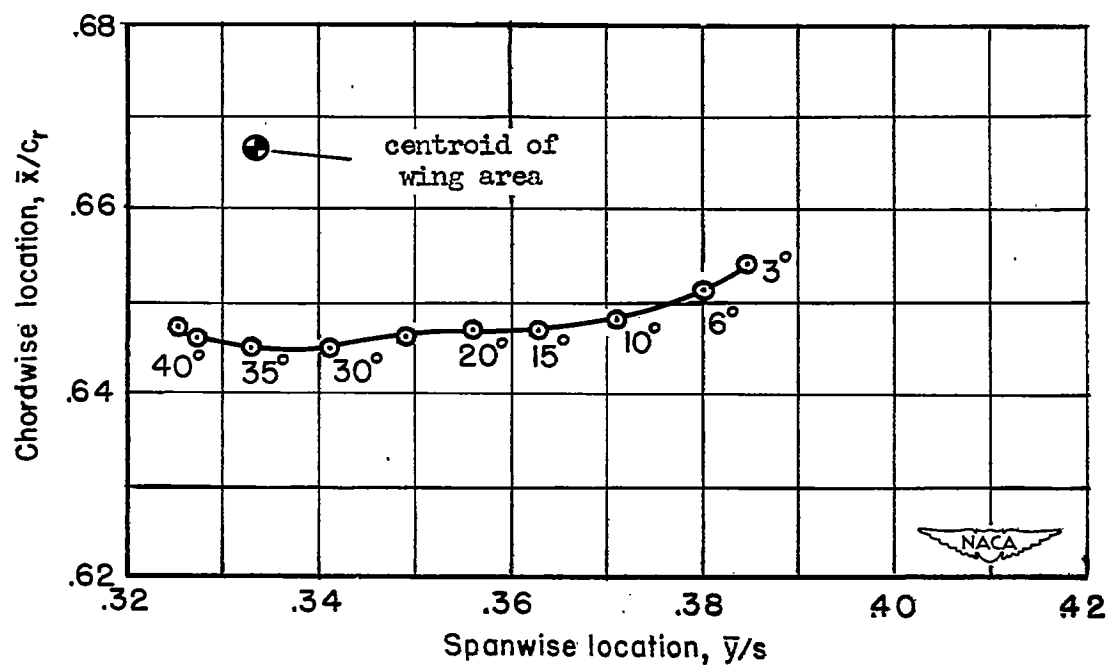
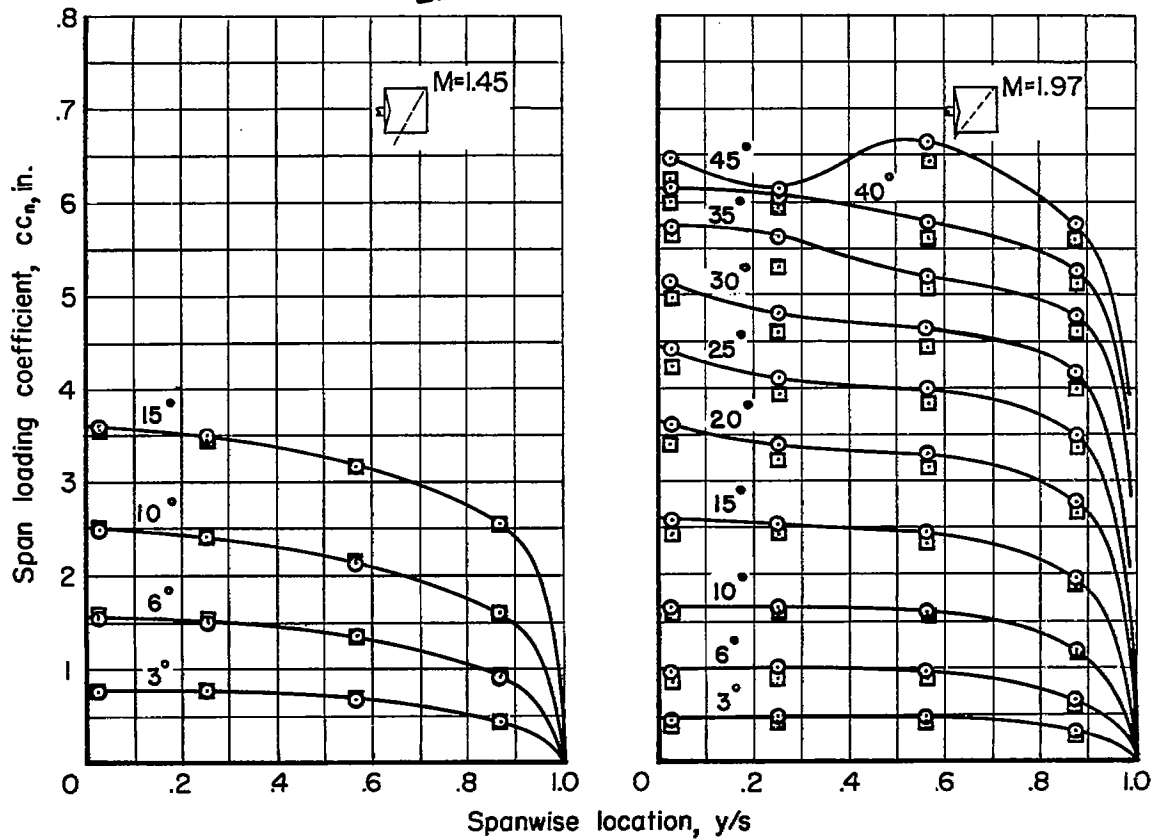
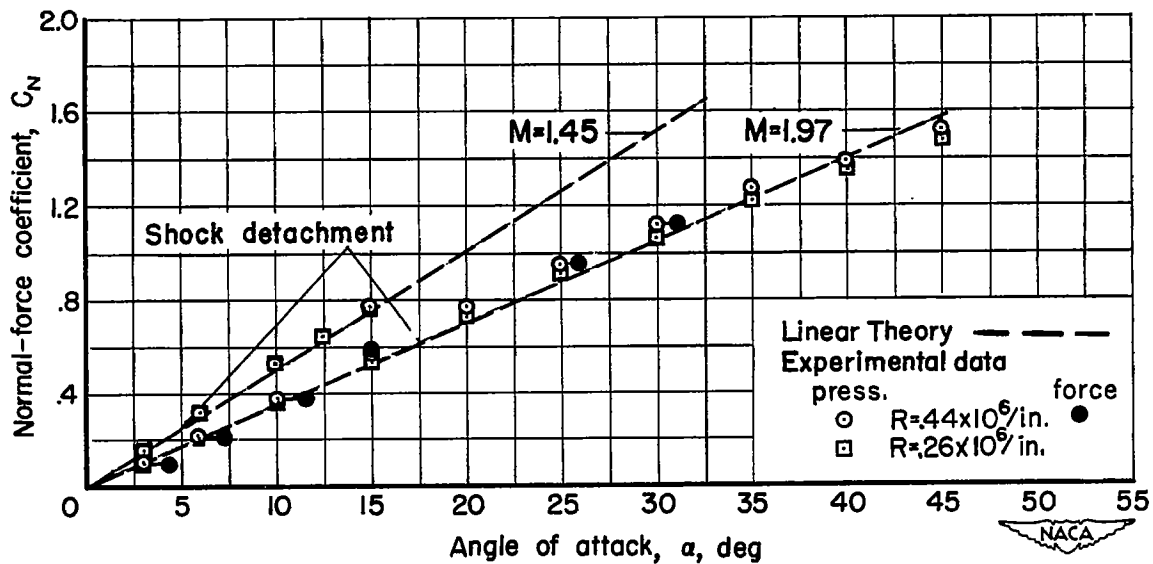
(c) Center-of-pressure position; $M = 1.45$.(d) Center-of-pressure position; $M = 1.97$.

Figure 3.- Concluded.

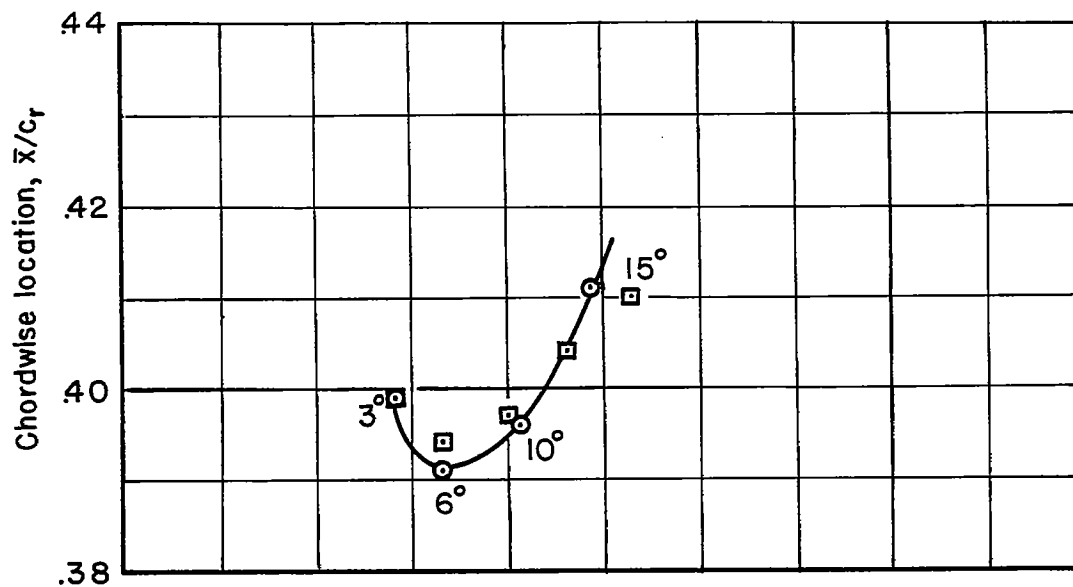


(a) Span loading.

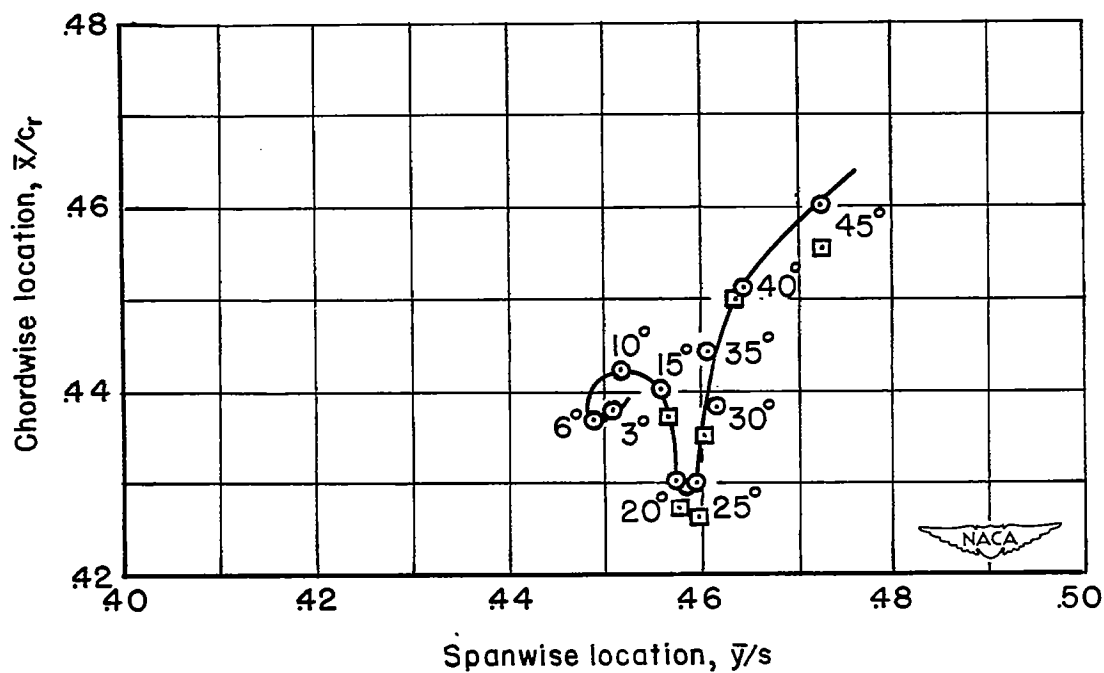


(b) Normal-force curves.

Figure 4.- Aerodynamic characteristics of wing 3.



(c) Center-of-pressure position; $M = 1.45$.



(d) Center-of-pressure position; $M = 1.97$.

Figure 4.- Concluded.

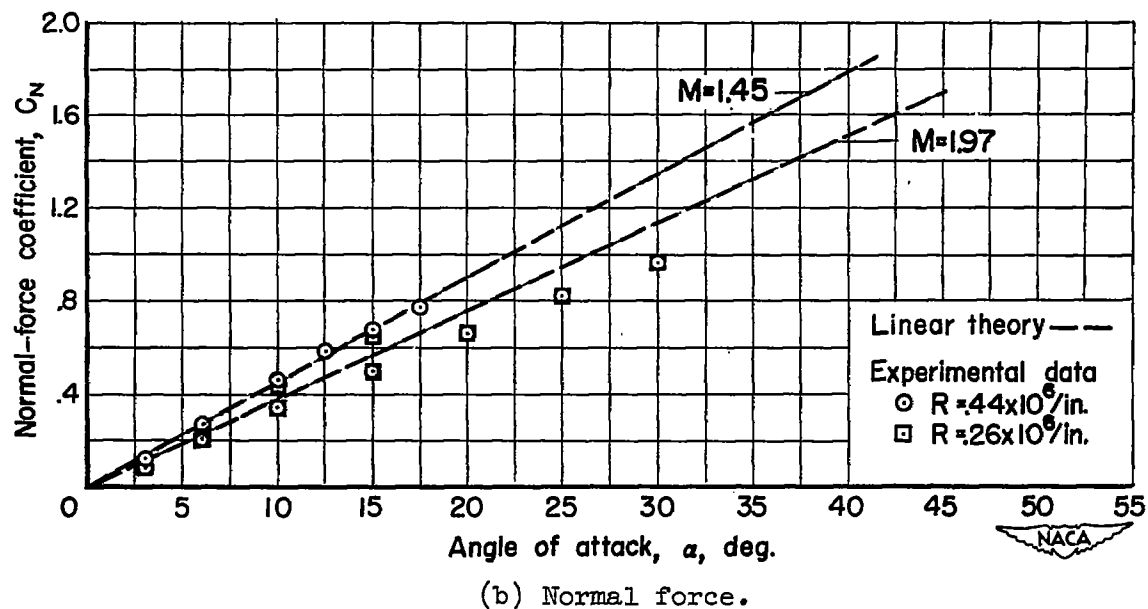
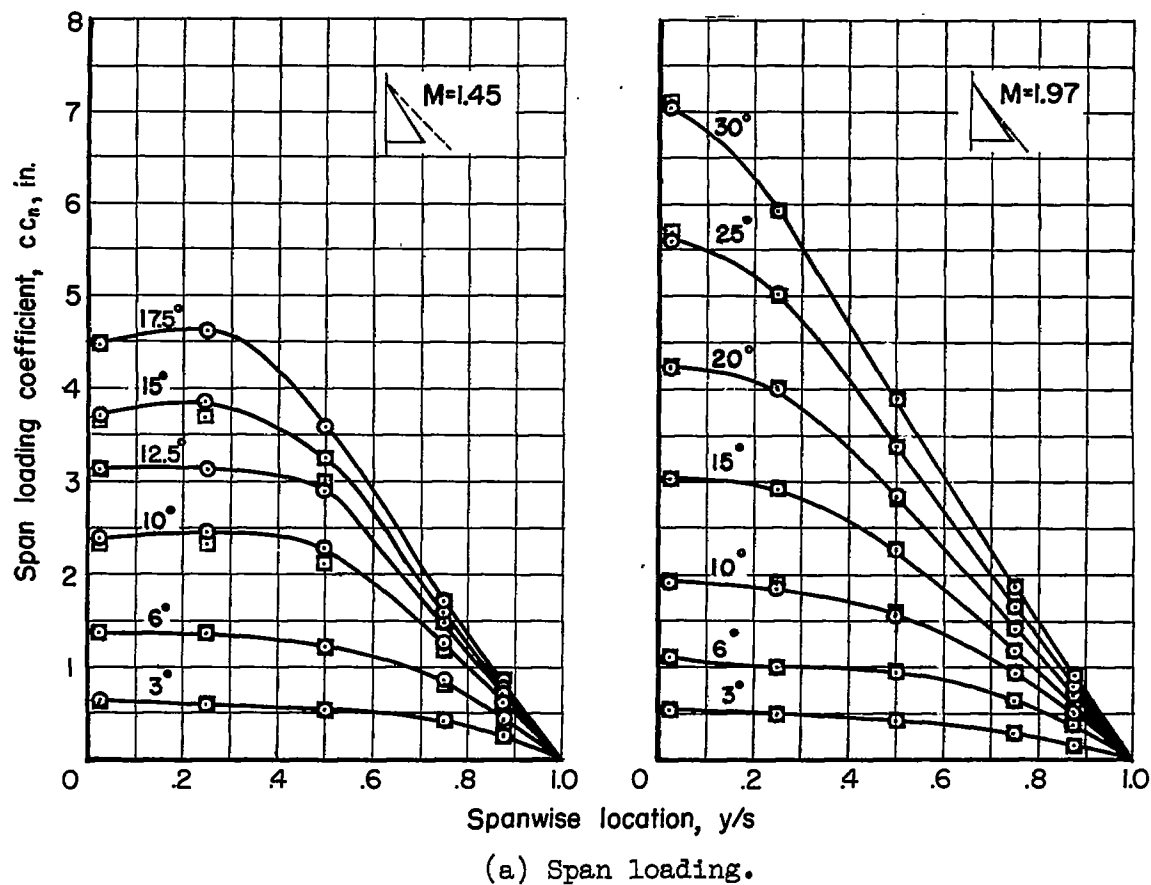
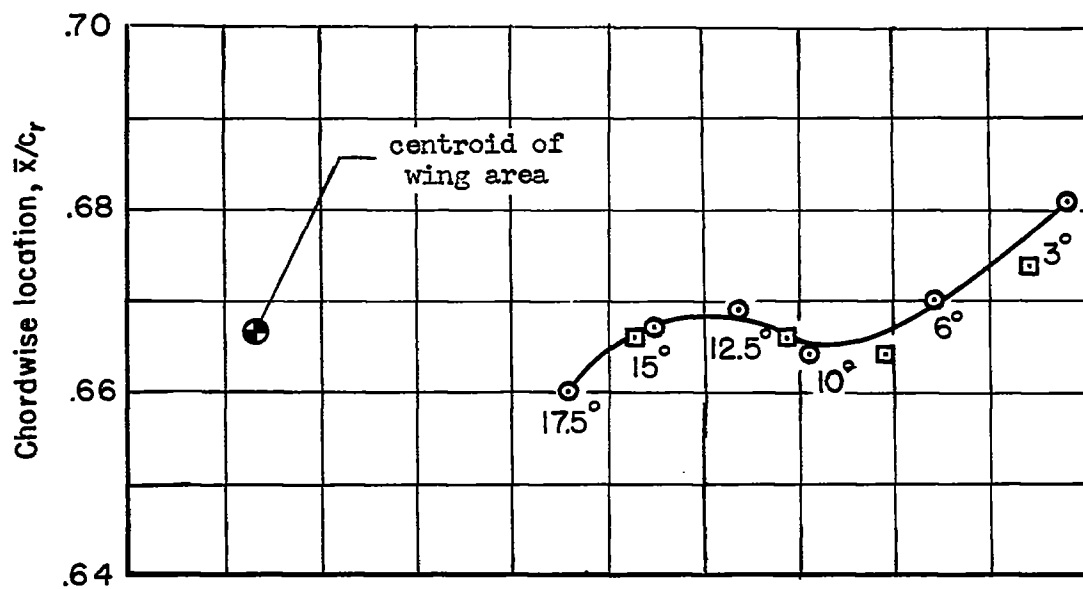
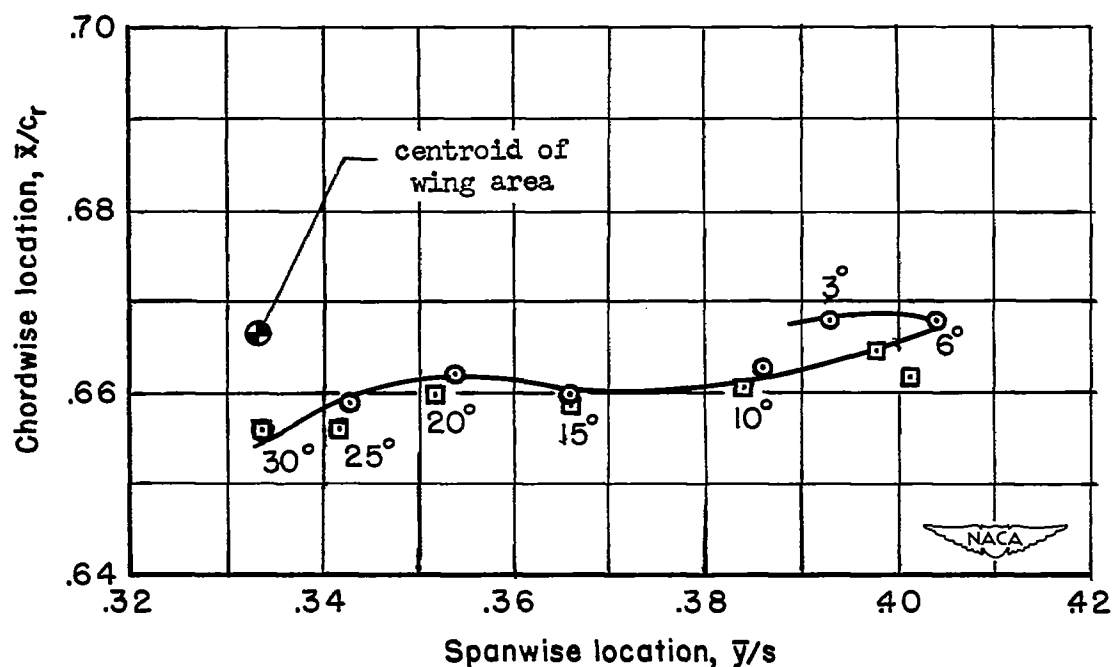


Figure 5.- Aerodynamic characteristics of wing 4.

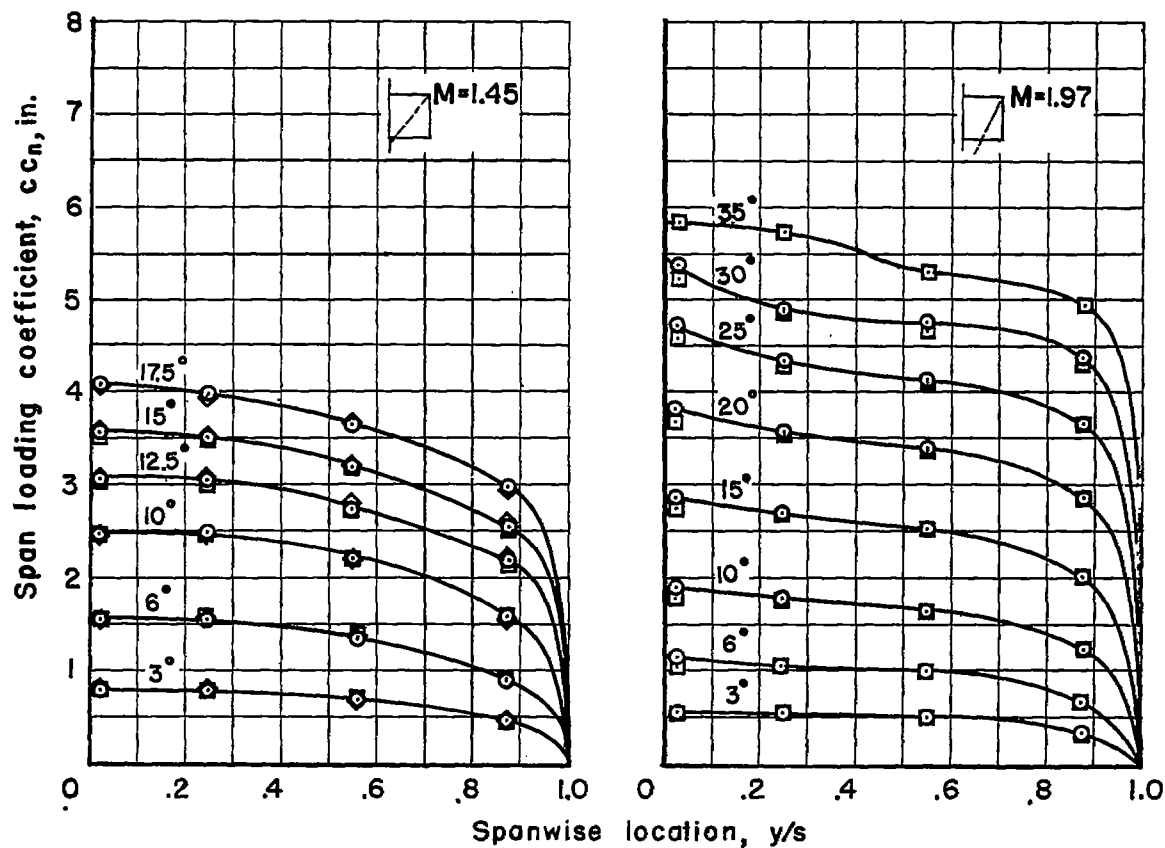


(c) Center-of-pressure position; $M = 1.45$.

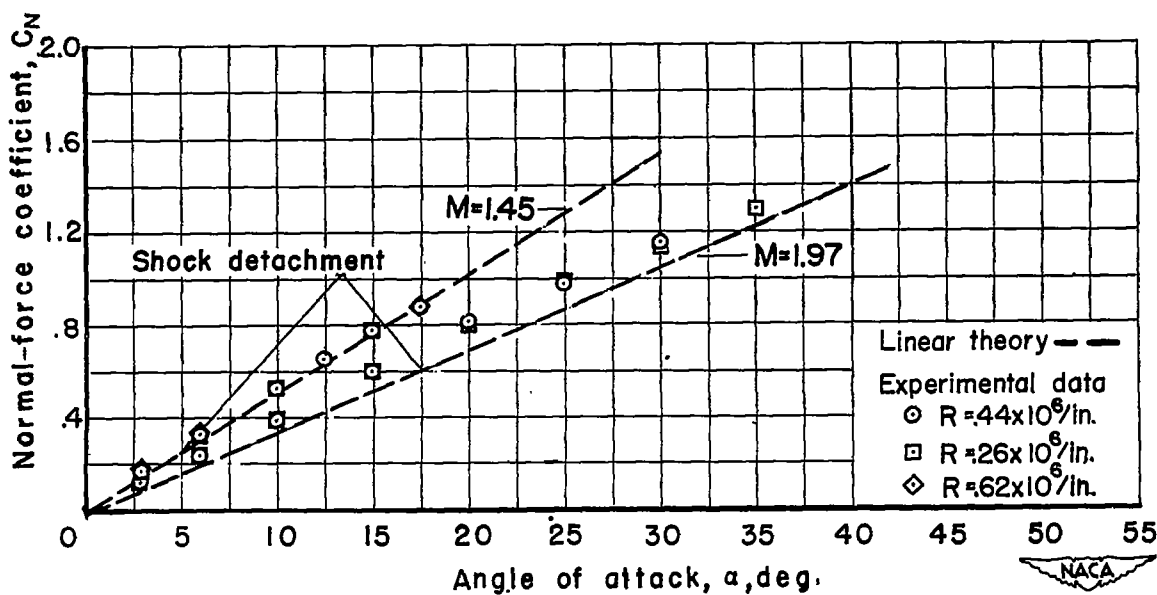


(d) Center-of-pressure position; $M = 1.97$.

Figure 5.- Concluded.



(a) Span loading.



(b) Normal-force curves.

Figure 6.- Aerodynamic characteristics of wing 5.

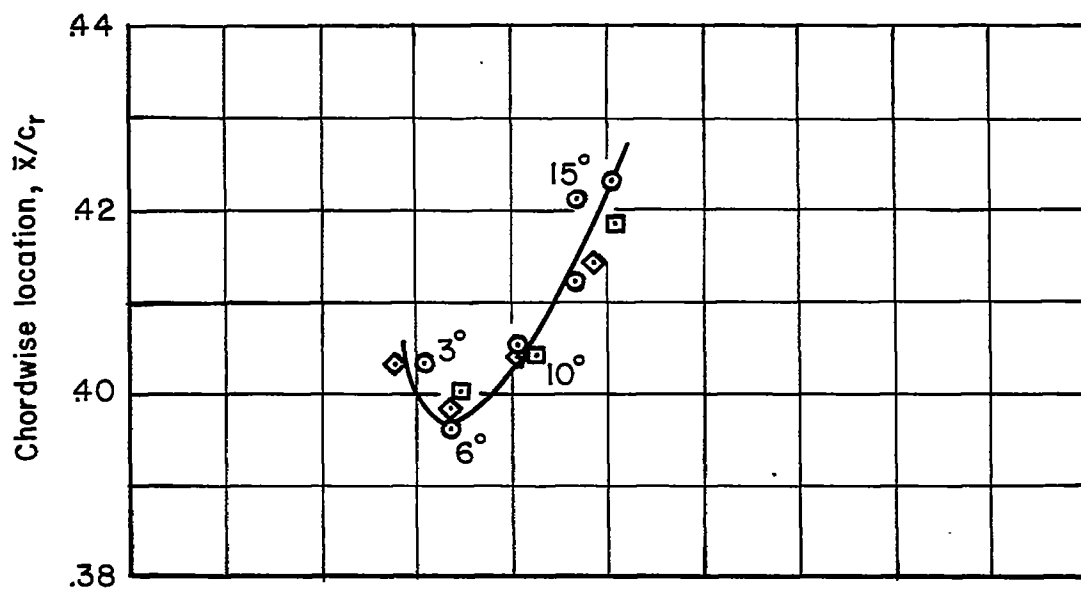
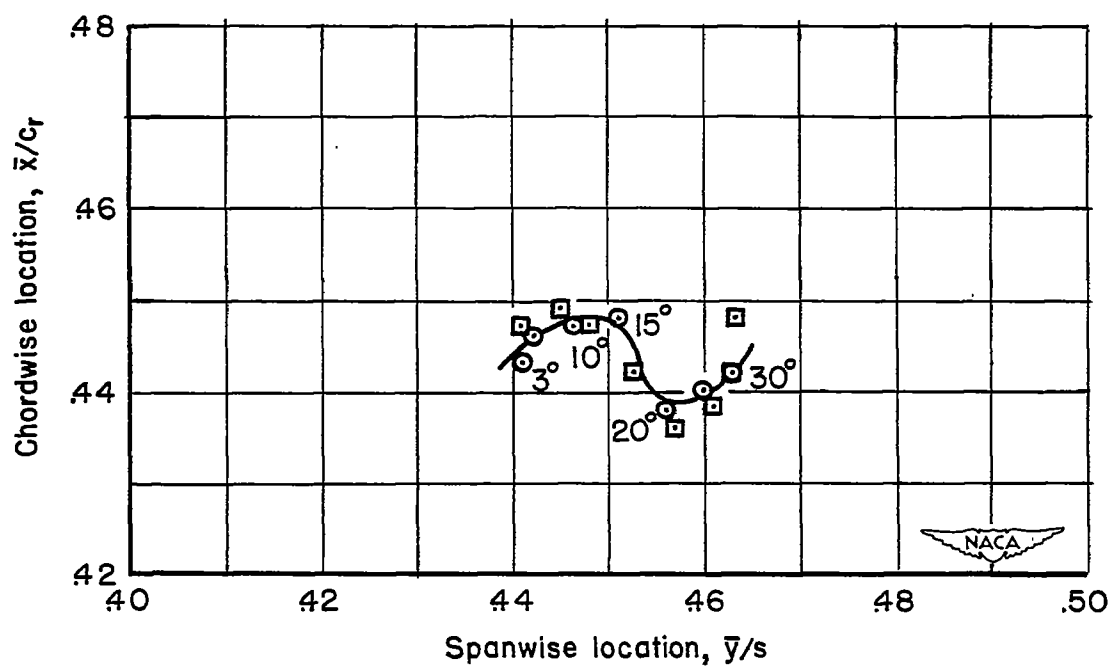
(c) Center-of-pressure position; $M = 1.45$.(d) Center-of-pressure position; $M = 1.97$.

Figure 6.- Concluded.